An-Najah National University

Faculty of Graduate Studies

Effect of Horizontal Eccentricity on the Response Reduction Factor (R)

By

Haya Abd El-Hadi Butami

Supervisors

Dr. Mohammad Samaaneh

Dr. Monther Dwaikat

This Thesis\Dissertation is submitted in Partial Fulfillment of the Requirements for the Degree of Master\PhD program name, Faculty of Graduate Studies, An-Najah National University, Nablus - Palestine.

202

Effect of Horizontal Eccentricity on the Response Reduction Factor (R)

By

Haya Abd El-Hadi Bustami

This Thesis was Defended Successfully on 00/00/0000 and approved by

Insert Name	_____
Supervisor	Signature
Insert Name	_____
Co-Supervisor	Signature
Insert Name	_____
External Examiner	Signature
Insert Name	_____
Internal Examiner	Signature

Dedication

I dedicate this thesis to my beloved family, whose steadfast support, encouragement, and sacrifices have been fundamental to the successful completion of this work.

Furthermore, I dedicate this work to my doctors. Their guidance, constructive feedback, and inspiring mentorship have supported the quality and depth of this research.

Acknowledgements

Praise is to Allah, first and foremost. I would like to express my sincere gratitude to my supervisors, Dr. Mohammad Samaaneh and Dr. Monther Dwaikat, for their valuable guidance throughout this thesis.

I would also like to extend my heartfelt thanks to my family for their support and understanding of my academic journey.

Declaration

I, the undersigned, declare that I submitted the thesis entitled:

Effect of Horizontal Eccentricity on the Response Reduction Factor (R)

I declare that the work provided in this thesis, unless otherwise referenced, is the researcher's own work and has not been submitted elsewhere for any other degree or qualification.

Student's name _____

Signature: _____

Date: _____

List of Contents

List of Tables

List of figures

List of Appendices

Effect of Horizontal Eccentricity on the Response Reduction Factor (R)

By

Haya Abd El-Hadi Bustami

Supervisor

Dr. Mohammad Samaaneh

Dr. Monther Dwaikat

Abstract

Structural irregularities significantly affect the seismic performance of buildings. Structures with architectural flaws may endure excessive twisting, differential story displacements, and probable collapse during seismic events. International standards, including ACI and ASCE, lack explicit directives for including the response modification factor (R) in the presence of horizontal eccentricity cases. The study aims to examine the impact of horizontal irregularity on the R factor for Intermediate Moment Resisting Frame (IMRF) structures. The study examines two variables: the number of stories and the amount of eccentricity. The study encompasses structures of 5, 7, 9, 12, and 15 stories, exhibiting eccentricity indicator values that vary from zero for reference specimens to 60% of the building width. SAP2000 is utilized for the analysis and design of buildings, incorporating response spectrum nonlinear analysis for seismic forces in accordance with ASCE standards. Push-over curves are produced to ascertain the correlation between horizontal eccentricity and R-value. Diverse push-over curves are utilized to examine various conditions. This encompasses standard push-over curves with flexural hinges, push-over curves incorporating mixed flexural, shear, and torsion hinges, as well as push-over curves reflecting the influence of bidirectional lateral pressures (push-over modal curves). The results demonstrate that the R-factor for the reference building corresponds with the recorded code value. Moreover, elevated eccentricity levels diminish the R-factor for buildings of identical height. As the elevation of the structure rises, the R-factor diminishes. The R-factor reduction varies from zero for the reference specimens to 25% for a fifteen-story with 60% eccentricity indicator. Utilizing bidirectional push-over curves that integrate integrated flexural,

shear, and torsion hinges results in a 30% reduction in R-factors. For the majority of moderately tall structures, the reduction is approximately 15%. The decrease in the R-factor results from the development of plastic hinges on one side of the structure, causing abrupt failure of specific joints before the joints on the opposite side give.

Chapter One
Introduction and Theoretical Background

1.1 Motivation

Natural disasters have escalated globally, as reported by the Centre for Research on the Epidemiology of Disasters (CRED). Appendix 1 illustrates the frequency of disasters over the past century, clearly indicating a substantial rise in their occurrence. Researchers across several disciplines are endeavoring to comprehend the origins and mitigate the impacts of these catastrophic catastrophes on human life. Earthquakes are among the most significant events, resulting in extensive devastation of structures annually across various regions of the globe. Consequently, standards and specifications are always evolving design protocols and underscoring the significance of seismological investigations to enhance the safety of structures and individuals.

Seismic design methodology is entirely force-centric. The force-based design depended on the base shear force derived from dynamic seismic motion, utilizing the acceleration response spectrum and the anticipated elastic period of the structure. (A. Elattar, A. Zaghw, and A. Elansary, 2012). The seismic force in the design is contingent upon the structural system and the degree of details. The seismic design codes delineate these aspects as particular criteria for value estimation. The seismic design methodology in Palestine lacks precision due to the absence of a specialized code for Palestinian engineers, stemming from constrained resources and inadequate development; thus, parameter values are derived from worldwide codes, which may not be appropriate for certain typical structures.

Structures in Palestine exhibit a lack of uniformity and irregularity, particularly in the spacing between columns, which significantly impacts the relative stiffness of beams and columns inside the frames. Consequently, it is imperative to examine the legitimacy of building code criteria for application in Palestine. Asymmetric structures have gained prominence in the realm of architecture. Individuals globally endeavor to construct distinctive edifices. The asymmetric structures introduce horizontal eccentricity in the building, necessitating designers to devise solutions that comply with safety regulations.

It is illogical to presume that the structure will maintain elasticity under seismic forces. The nonlinear design is a complex process, and its impact can be assessed using a reduction factor known as the Response Reduction Factor (R). Structures in Palestine predominantly exhibit irregular configurations, with random column distributions and different span lengths, fulfilling diverse architectural functions. Consequently, the relative stiffness between the column and beam will alter. Currently, there are no rules regarding how the R-factor would be affected by alterations in column-to-beam relative stiffness. This study intends to investigate the validity of the code-provided R-factor estimates for various column-to-beam relative stiffness ratios. Numerous edifices in Palestine are classified as horizontally irregular structures based on the distribution of columns, varying span lengths, the positioning of shear walls, and architectural objectives. Consequently, the narrative rigidity will undergo a significant alteration. Currently, there are no definitive standards regarding the impact of torsional irregularity on the response reduction factor. This study seeks to investigate the R-factor values for different levels of torsional irregularity in buildings.

The research investigates several structures comprising 5, 7, 9, 12, and 15 stories, with an eccentricity indicator ratio ranging from 0L to 0.6L based on the structure's eccentricity indicator. The study seeks to define the correlation between the torsional eccentricity ratio and the response reduction factor (R). The analysis will utilize Sap2000 to construct Moment Resisting Frame (MRF) structures and get precise outcomes via non-linear analysis.

1.2 Perspective from Design Codes

The principle of seismic design codes is to diminish the design seismic force based on ductility considerations. The identical process is employed across several codes, albeit with varying reduction percentages contingent upon the frame type and reconnect features. Codes underscore the significance of the decrease percentage that maintains structural safety. In American codes, the response modification factor (R-factor) serves as a metric to denote the attenuation of seismic forces across several frame categories. These categories are prevalent in worldwide building regulations, but with varying nomenclature and R-factor values. Any modification to the building's structural elements can influence its behavior, hence

affecting the R-factor. This section examines torsional irregularity and the methods for calculating the reduction factor in accordance with current design codes.

1.2.1 Eccentricity and Torsional irregularity

The response of structures to earthquakes is governed by several parameters, including mass, stiffness, and strength. Structural failure from seismic forces typically initiates at points of vulnerability within the edifice. These deficiencies primarily arise from inconsistencies in stiffness, strength, and mass.

Any structural analysis aims to identify the optimal design that guarantees safety while minimizing costs. Calculating the center of mass and center of stiffness is one of the initial tasks in the design process. The center of mass, sometimes referred to as the center of gravity, is a theoretical place within a structure where the total weight is considered to be concentrated; at this point, the structure would maintain equilibrium in any orientation. The center of gravity of any structure can be determined from its layout. The center of rigidity is the stiffness centroid in floor-diaphragm layouts. The center of rigidity is defined as the point at which the structure exhibits completes resistance to rotation. Columns and shear walls are the primary elements that enhance the center of stiffness.

Eccentricity arises when the center of gravity of a building does not align with the center of stiffness. Eccentricity can generally be mitigated by enhancing the lateral stiffness along the column line through the implementation of retaining walls or braces, or by augmenting the column dimensions. Nonetheless, it cannot be universally circumvented in every instance. Asymmetric structures have gained prominence in the realm of architecture. Individuals across various regions globally endeavor to construct distinctive edifices. The asymmetric structures with horizontal eccentricity induce torsional irregularity in the building, necessitating the designer to implement a specialized design to meet safety standards.

Buildings experience both translational and rotating forces; however, when the center of mass aligns with the center of rigidity, only the translational component is evident. The rotational component is affected by eccentricity, which is the distance between the center of mass and the center of stiffness. Codes provide constraints on evaluating torsional irregularity based on the maximum and average drift of structures.

Torsional irregularity possesses multiple definitions and constraints as delineated by various codes. The American Society of Civil Engineers (ASCE) code defines torsional irregularity as a condition in which the maximum story drift of a structure exceeds 1.2 times the average story drift ($d_{max}/d_{avg} > 1.2$). Story drift refers to the vertical displacement of a floor level of a building in relation to the adjacent levels above or below the specified floor level, as seen in figure 2. Drift can be succinctly defined as the horizontal displacement of a building relative to its foundation when subjected to lateral forces, such as wind and seismic loads.

The Uniform Building Code (UBC) delineates torsional irregularity in a manner analogous to the ASCE code when diaphragms exhibit rigidity. Torsional irregularity should be assessed when the largest narrative drift exceeds 1.2 times the typical tale drifts. The Turkish code restricts torsional irregularity in structures when the torsional irregularity factor surpasses 1.2. Nonetheless, the regulation mandates a revision of the structural system when the torsional irregularity factor surpasses a value of 2. The European code addresses torsional irregularity when structural eccentricity exceeds 30% of the torsional radius ($e_{0X} \geq 0.30r_X$, $e_{0Y} \geq 0.30r_Y$) and the building's slenderness ratio is greater than 4 ($\lambda = L_{max}/L_{min}$). In the Japanese code, the story drift limit under seismic shear force for the serviceability limit state must not surpass 1/200 (0.005) of the story height. The value rises to 1/120 (.0083) for non-structural elements. Torsional irregularity poses a concern for buildings when lateral drift surpasses code limitations. However, this will impact constructions with additional force components due to torsion, hence affecting the structural response.

1.2.2 Response reduction factor

The structure will not remain in the elastic phase under seismic demands. The nonlinear design is a complex process, and its impact can be assessed using a reduction factor known as the Response Reduction Factor (R).

The R-factor denotes the ratio of the maximum lateral force that the structure can sustain elastically to the lateral force for which it has been engineered, as depicted in the index. The term R denotes the anticipated level of overstrength and ductility in a construction. The design of the structure can accommodate a force lower than the anticipated seismic force by incorporating the overstrength factor (RS), redundancy factor (Rr), and ductility factor ($R\mu$),

thereby averting structural collapse. The response reduction factor is defined as a function of these parameters, as seen in equation 1.

$$R=R_s R_\mu R_\xi R_r \quad (1.1)$$

- Redundancy factor R_r can be estimated as ratio of ultimate load to the yield load; the estimation requires detailed non-linear analyses

  $$R_r = V_u/V_y \quad (1.2)$$

- Ductility factor R_μ is used to reduce the strength of elastic force (V_e) to the ideal level of yield strength (V_y) of the structure, which can be calculated as following

  $$R\mu = \frac{Ve}{Vy} \quad (1.3)$$

- The over-strength factor R_s represents the additional strength of the structure which has beyond the design strength. The additional strength exhibited by structures may be due to various reasons, such as sequential yielding of critical points, factor of safety considered for the materials, load combinations considered for design and member size ductile detailing.
- Damping factor R_ξ is used for structures which have an additional energy dissipating (viscous damping) devices. So the buildings without viscous damping devices damping factor is 1, as the default code-based response reduction factors assume the inherent damping of structure 5% for critical damping case, so no extra modification is needed.

R-factor can be taken from the ASCE code according to the seismic force-resisting system as described in code tables. R values for moment resisting frame systems table is attatched in Appendix B. The value of R, used for design in the direction under consideration shall not be greater than the least value of R for any of the systems used in that direction.

The situation in the Euro code depends on the reduction of the elastic spectral demands to the strength design level using a period-dependent response factor, called the behavior factor q_o. This behavior is a function of ductility, building strength, structural system and stiffness regularity as shown in equation 1.4

$$q = q_o \times K_D \times K_R \times K_w \quad (1.4)$$

where;

q_o: The basic value for response factor.

k_D: Represent ductility class.

k_R: Is a factor reflecting structural irregularity in elevation.

k_W: Reflects prevailing failure mode (for MRF K_W is taken to be 1).

The values can be taken from the tables as shown in appendix A.

The IBC Code 83 specifies response modification factors for each type of framing system, as detailed in IBC 2012/ASCE 7-10 Table 12.2-1. The factors encompass R=5 for reinforced concrete Intermediate Moment Resisting Frames (IMRF). In contrast, UBC 97 has an R-Factor of 5.5 for the identical lateral resisting system. The R-factor values recommended in UBC 97 for moment-resisting frame systems range from 3.5 to 8.5, as indicated in the table in Appendix B. The Egyptian code addresses the R-values in Chapter 8, titled "Loads and Forces on Structural and Nonstructural Systems." In the Egyptian code, R-values for reinforced concrete structures can be designated as either 5 or 7 for RC moment-resisting frames, depending on the extent of ductility. The Egyptian coding table is referenced in Appendix B.

1.3 Literature review

1.3.1 General

Some non-symmetric architectural designs create significant eccentricity in buildings, prompting designers to implement specialized seismic designs to mitigate earthquake risks.

The structural field has several studies about the relationship between the torsional irregularity and the seismic parameters; no specific study has clarified a formula that links eccentricity to the response reduction factor.

The previous section provided an explanation of the code categories that address the torsional irregularity resulting from horizontal eccentricity, along with an explanation of the response

reduction factor. This section reviews the previous research related to the relationship between horizontal eccentricity and the response reduction factor.

1.3.2 Previous studies on the torsional irregularity and horizontal eccentricity

Xuanhua Fan, Jiacong Yin, Shuli Sun, and Pu Chen investigate an alternative methodology for calculating seismic response using accidental eccentricity. The study suggested that the RRP-MRSA method is a more rapid and efficient alternative to conventional spectral analysis for the seismic evaluation of buildings with unintentional horizontal eccentricity.

H. Gokdemir examines the impact of torsional irregularity on structures in seismic events. H. Gokdemir concludes that the eccentricity between the center of mass and the center of stiffness induces torsion in structures. The magnitude of the torsional moment is a function of the eccentricity ratio; enhancing the strength of structural elements in the weak direction of the building or reducing the strength of structural elements in the strong direction can mitigate the impacts of torsion on buildings.

Pengyu Sun, Weiping Wen, and Siwei Zhang conducted a study titled “Effects of Aftershocks on the Seismic Performances of Reinforced Concrete Eccentric Frame Structures.” It was discovered that horizontal eccentricity substantially diminishes the seismic capability of a structure. For instance, a 30% eccentricity results in diminished seismic resistance coupled with an escalation in torsional effects and residual displacements within the structure.

A recent study by Osman Akyürek and Hakan Ulutaş emphasized those standard code-based methodologies, which presume a constant accidental eccentricity ratio (e.g., 5% or 10% of the building dimension), may not adequately reflect the actual impact on the structure. The authors present an equation that relates the ratio of torsional to translational frequencies to the radius of gyration within the structure, providing a more accurate estimation of torsional eccentricity.

Furthermore, Ali Demir and M. Uzun conducted study on the effects of torsional irregularity related to site classes in multistory structures, revealing that the geometric design of structures should be symmetrical to minimize the torsional irregularity coefficient. If the plan geometry is not symmetrical, eccentricity values can be mitigated by using shear barriers. The base shear pressures in the building with torsional irregularity escalate with an increasing number of stories.

Meenkashi V. Landge and Fatemeh Aliakbar elucidate the impact of torsional irregularity in response spectrum analysis of building structures, concluding that various methods have been proposed and evaluated to ascertain the ratio of maximum to average story drift, thereby identifying the torsional irregularity of structures in response spectrum analyses. The research indicated that for structures with regular geometry and uniform stiffness, a minor mass eccentricity markedly amplifies floor response spectra. Furthermore, real structures may exhibit considerable discrepancies in mass, stiffness, and strength, leading to an exacerbation of floor response spectra.

Gunay Ozmen presented a paper addressing excessive torsional irregularity in multi-story constructions, aiming to establish a correlation between the torsional irregularity coefficient and the number of storeys. The research indicates that the torsional irregularity coefficient escalates as the number of stories diminishes for a standard structural group. Secondly, the peak values of torsional irregularity were attained when the walls were positioned near the center of gravity without corresponding with it. The maximum effect of increased eccentricity was determined to be 20%.

Additional researchers, including Pedram Omidian, Esra Ozer, Mehmet Inel, and Bayram TanikCaycia, have also examined the effects. Omidian examined the investigation of seismic performance of reinforced concrete structures including Shape Memory materials. Alloy rebar in cases of regular, torsional irregularity, and extreme torsional irregularity demonstrates that the incorporation of SMA in irregular structures alleviates the detrimental impacts of irregularity, including a decrease in base shear and drift. Ozer and her collaborators examine the seismic performance of lead-core rubber elastomeric bearings (LRB) and curved surface friction pendulum sliders (FPS). The findings demonstrate that the torsional irregularity coefficient values for lead-core rubber elastomeric bearing models with 20% eccentricity were, on average, 47% more than those for models without eccentricity.

A. Balaji Rao did research to examine the modification of mode shapes in irregularly built buildings. Rao endeavored to examine the optimal placement and configuration of structural walls for several torsionally irregular buildings. A comparative analysis was conducted to determine the optimal placement of shear walls that reduces torsional displacement and establishes the translational mode as the fundamental mode.

The influence of torsional irregularity in structures, as emphasized in prior publications, is substantial and cannot be overlooked in design considerations. Torsional irregularity necessitates specialized structural designs employing sophisticated methodologies that require a specific budget; hence, if torsional irregularity can be mitigated, the design process becomes more straightforward. Although it may not be feasible to eradicate torsional irregularity, the design must be underpinned by suitable specifications.

Other studies, such as Jagat Kumar Shrestha, endeavor to determine the response reduction factor for masonry buildings, assessing various mechanical features utilized in contemporary codes to mitigate the elastic response of the structure. The researcher concludes that the R-value specified in IS: 1893-2016 for unreinforced masonry is not advisable for random rubble stone masonry structures utilizing mud mortar.

Divya Brahmavrathan and Sharjuban both conducted a study of the seismic response reduction factor for vertically uneven reinforced concrete structures. In setback buildings, the value of the response reduction factor escalates with an increase in the number of floors. Juan Carlos Perez and his associates employed the FEMA P-695 methodology to assess the response reduction factors of irregular reinforced concrete structures. Juan concluded that the value stipulated by the Venezuelan seismic code (R = 6) is secure for the analyzed structure. The response reduction factor for horizontally uneven buildings is a significant parameter.

Bholebhavi Rahul D and Inamdar V.M. authored a paper on the response reduction factor for asymmetrical buildings. The article concludes that when the sudden vertical or horizontal irregularity increases, the response reduction factor decreases. Despite acknowledging the researchers' efforts, none of the current studies have investigated the correlation between torsional irregularity and the response reduction factor (R), which is regarded as a supplementary component for achieving a comprehensive approach to seismic design approaches.

Torsional irregularity significantly influences structural design. Contemporary advanced analytical software can manage any level of torsion, whether it is a standard or an excessive irregularity. According to rules, any structure designated as SDC E or F must not exhibit extreme torsional irregularity; therefore, the design must be modified accordingly. Assignment of SDC E or F is applicable to buildings exhibiting long-period spectral accelerations (S1) of 0.75g or

above. Furthermore, sites located in densely inhabited areas with moderate to high seismicity must consider excessive torsional irregularity.

In the ever-evolving domain of seismic design, only time will disclose the trajectory of forthcoming spectral acceleration maps. Designers of structures in seismic regions must remain acutely aware of modifications to these parameters, since this matter carries significant ramifications and associated constraints for specific abnormalities.

1.4 Problem statement

Upon examining the international code and prior research, the significance of the R-factor in earthquake design is unequivocal. Furthermore, the R-factor alters as the structural system of building changes, making it essential to examine how the R-factor is affected by variations in the features of the frame.

The R-factor is contingent upon the attributes of each structure. Limiting the R-value to overall ductility and natural period constitutes an oversimplification. To achieve a more precise R-factor, additional structural details must be incorporated into the calculations.

Contemporary seismic design programs incorporate the nonlinear response of a structure implicitly via R. The factor allows designers to execute a linear elastic force-based design while considering nonlinear behavior and deformation constraints. The influence of horizontal eccentricity on structures is not explicitly discussed. This research examines the impact of horizontal eccentricity on the R value for IMRF structures as the eccentricity indicator increases from 0L to 0.6L in increments of 0.1L for each scenario.

1.5 Study hypothesis

- The current research is limited to RC-IMRF structures.
- The rigidity of the infill is not taken into account in this investigation. However, the analysis assumes associated mass and weight.
- This study does not consider the impacts of soil-structure interactions.
- The program's capabilities ignore the contribution of shear from torsion on moment-curvature curves.

1.6 Importance of the study

The principal reference for the structural designer is the code. Codes emphasize seismic design; nonetheless, the impact of horizontal eccentricity on further seismic characteristics remains inadequately characterized.

The prevalent utilization of asymmetric structures, which can result in significant horizontal eccentricity, necessitates that designers adopt specialist seismic design strategies. Nonetheless, expertise regarding horizontal eccentricity design in the realm of seismic engineering is deficient.

1.7 Objectives

The main objective of this research is to investigate the effect of horizontal eccentricity on R for RC-MR buildings. The obtained value will be compared to ones that are provided by international codes. The study aims to satisfy this main objective through the following sub-objectives:

1. Development of push-over curves for multistory buildings using nonlinear software
2. Investigation of the effect of different values of horizontal eccentricity on R
3. Examination of the impact of building aspect ratio, in combination with horizontal eccentricity on R
4. Provision of clear guidelines for designer regarding effect of horizontal eccentricity on R

1.8 Methodology

Seismic forces play a vital role in the design of structures, and generally these forces are computed using the linear static method with the aid of a response reduction factor. The R-factor incorporates the nonlinear response of any structure during a seismic event, allowing the designer to use a linear force-based design while considering the structure's nonlinear behavior and deformation limits.

After reviewing previous research, researchers notice the clear effect of horizontal eccentricity on the response reduction factor. The studies explain that as the horizontal eccentricity in the structure increases, the response reduction factor decreases.

As mentioned before, the knowledge of the horizontal eccentricity effect on R is not enough. For that reason, a non-linear finite element model will be established with simple cases of frames. Then, analytical models of Moment Resisting Frame (MRF) structures of different stories with horizontal eccentricity will be used in this study. The analysis for this thesis will be done using a computer program to calculate R values for each model so there is a clear comparison between R values with and without horizontal eccentricity.

In this thesis, the models will follow the code limitation for categorizing them as MRF systems. According to that, certain structural height limitations must be considered. The structures will have varying story numbers, each with specific horizontal eccentricity values.

After obtaining reliable results from both hand calculations and computer program outputs, clear designing steps will be outlined to explain the relationship between the horizontal eccentricity and the response reduction factor. The study will be conducted following the below steps:

a) Extend the literature review for detailed studies and methodology of previous research.
b) Develop non-linear finite-element models and verify models from simple cases, and extend the verified models to the cases of interest.
c) Define the parameters of interest and the range of variables.
d) Conduct the parametric study to investigate the effect of horizontal eccentricity on R.
e) Analyze the results and define the effect of R based on the parameters.
f) Summarize the key points and provide recommendations.

1.9 Thesis outline

The thesis is organized in four chapters as follows:

Chapter 1 (Introduction and Theoretical Background) presents the introduction, background and study motivation. Then move to talk about the design codes and previous literature reviews. Finally, a brief preview is given for the importance, objectives, and methodology of the study.

Chapter 2 (Methodology) describes the modeling aspects of horizontal eccentricity and the geometries considered in this study. Also, this chapter presents the methods that were used in the modeling and analysis of buildings.

Chapter 3 (Results) starts with a presentation of the results of the response reduction factor and compares them with the results of the ASCE 7:16 code.

Chapter 4 (Conclusion and Future Work) contains the discussion of the results. There is also a section to offer significant findings and conclusions of the study and the future work.

Chapter Two
General Analysis procedure

2.1 Non-linear analysis

2.1.1 Static pushover analysis

The pushover method is preferred due to its simple procedure; it also indicates the real behavior of the structure and the effect of plasticity in the members on the structure's response. Pushover analysis can be a force-controlled performance or displacement-controlled performance depending on the physical nature of the load and the expected behavior of the structure. The force-controlled method is used when the load is known, while the displacement-controlled method is used when specified drifts are sought, as in seismic loading, where the applied load is unknown, or when the structure can be expected to lose strength or become unstable.

The push-over analysis methods (PO) can also be divided into three general groups:

- The conventional pushover methods can be categorized into the following types:
    - Capacity Spectrum Method, CSM
    - Improved Capacity Spectrum Method, ICSM
    - Displacement Coefficient Method, DCM
    - Modal Pushover Analysis, MPA
- The Adaptive pushover methods
- The pushover methods focus on energy.

To compare the results from different PO methods Mohssen Izadinia et al. (2011) studied the response modification factor for steel moment-resisting frames using different pushover analysis methods. The study indicates that the maximum relative difference for response modification factors was about 16%, obtained by the methods of conventional and adaptive pushover analysis. Izadinia provides that the various techniques of P.O. analysis can be trusted to produce similar results.

The main advantages of pushover modal analysis include

- Improving accuracy in capturing the seismic response of irregular structures.
- Pushover modal analysis improves the estimation of displacement and force demands throughout the structure's height.
- This approach allows for a more realistic assessment of damage progression, particularly in higher mode-dominant structures.

Despite its usefulness, pushover analysis remains an approximate method. It does not capture cyclic degradation, dynamic amplification, or the full range of soil-structure interaction. Hence, while it is suitable for preliminary assessment and performance-based design, results should be interpreted with caution.

In this study, the pushover analysis approach was adopted to evaluate the structural response, with additional procedures such as load normalization to enhance result accuracy, particularly for torsionally irregular models.

2.1.2 Non-linear procedures

Most of the building codes have four levels of design analysis as follows:

- Linear static analysis (LSP)
- Linear dynamic analysis (LDP)
- Nonlinear static analysis (NSP)
- Nonlinear dynamic analysis (NDP).

The designer uses the linear static analysis when the structure is regular with limited height. Both LSP and LDP use elastic analysis to determine the internal forces. The technique of determining which method to use depends on the basic level of forces and the distribution along with the structure’s height.

When the structure moves to inelastic behavior, nonlinear methods must be used. The non-linear PO is an incremental analysis which divides the applied load and target displacement to the predefined number of steps. The applied loads increase or decrease to achieve the required displacements. The stress and deformation output from the previous step will be imposed on the next step of loading. The process is repeated until the instability of the

structure or target displacement; in other words, the process is repeated until failure. The NDP is based on combining transient time history and the inelastic behavior of the structure. The finite element software SAP 2000 generates the resulting nonlinear static behavior of the structure through incremental analysis, assuming elastic behavior between each increment where plastic hinges form at each increment. (Zaid, 2018)

The damage level in the structure can be indicated by the displacement of the resulting load response curve, which is called the capacity response curve. The curve value and shape depend on the strength, stiffness, and sequence of the plastic hinges and distribution of ductility of the members in the structure.

Nonlinear analysis can be done using computer programs like Etabs and Sap2000, which model the nonlinear behavior and directly perform the pushover analysis to create a capacity curve of the structure. A displacement-controlled analysis done on computer program as the following steps

- Create a three-dimensional model to represent the RC building frame.
- Add the gravity and live loads
- Application of 10% static lateral load induced due to earthquake, at CG of the building
- Developing M-θ relationship for critical regions (Plastic hinging zone)
- Pushing the structure using the static lateral loads patterns, up to displacements larger than those associated with target displacement using static pushover analysis
- Developing a hinge-progressing sequence

To have correct results from the PO analysis, the structure has to be controlled by a major fundamental mode during the EQ.

2.1.3 Local nonlinear behavior

Nonlinearity of materials and members occurs when the material's strain or the member's deformation increase the structure's deformation as the corresponding stress and restoring force are no longer proportional to the strain or deformation. In other words, a nonlinear stress-strain or force-deformation curve comes into view.

In the seismic design, high stress and force will not be generated when the structure has large displacement due to large earthquake motion; because of that, the softening type of nonlinearity is favorable in the structural seismic design. Exceptionally, the hardening nonlinearity type is used for the high strain range, as in the seismic isolation bearing.

The nonlinear behavior of structural elements could be defined as follows:

- Continuous plasticity

  This approach occurs when the stress-strain law is updated at every member's location. A 3D material modeling must be done to reach the required level of modeling or a simplifying section fiber approach. The section fiber method is a very accurate procedure, but it is computationally expensive. The fiber element procedure obtains nonlinearity on the cross-sectional level, and then the overall nonlinear behavior is interpolated along with the member.

- Concentrated plasticity

  In this case, the plastic behavior is assumed to occur in a specified location with a concentrated inelastic deformation at the plastic hinge position.

2.2 Response reduction factor

2.2.1 Response reduction factor formula

As mentioned before, R-factor can be described as the product of the strength, ductility and viscous damping factors as shown in the equation

$$R=R_s \times R_\eta \times R_\xi \qquad (2.2.1)$$

Where,

R_s is the maximum shear factor divided by the design base shear factor (Vy/Vd)

R_η is the base shear divided by the yield base shear (Ve/Vy)

R_ξ is equal 1.0

ATC 19 splits R into three component factors, where R_ξ is replaced by R_R (redundancy factor). The equation become as follows:

$$R=R_s \times R_p \times R_R \quad (2.2.2)$$

Even for structures of the same type, the factor values in different codes vary slightly.

2.2.2 Overstrength factor

Overstrength is the additional strength beyond the design strength after the structure reached its final strength and deformation capacity. Structure designers use the overstrength factor to design more economical structures by reducing the loads used in the design.

The main sources of overstrength are

- Load factors and multiple load cases
- The difference between the actual and design material strength
- Participation of nonstructural elements
- Codes minimum required reinforcement and member sizes that may exceed the design requirements
- Actual confinement effects
- The difference between the actual and design material strength
- Serviceability limit state provisions

Member size or reinforcement that is larger than required, strain hardening in materials, confinement of concrete, strength contribution of non-structural elements, and special ductile detailing are also the sources of overstrength.

Overstrength factor (Ω) = apparent strength/design strength

$$\Omega = V_u/V_d \quad (2.2.3)$$

2.2.3 Ductility reduction factor

In the seismic design, structure strength, stiffness, and ductility are crucial properties that have to be studied well for the seismic protection. These properties are the reduction factor terms.

- Strength

  The structure must have adequate strength to resist internal actions generated during its elastic dynamic response. In other words, the structurally designed load must be larger than the seismic load.

- Stiffness

  In simple terms, stiffness is a measure of how flexible a member is. This means the extent to which the element is able to resist deformation or deflection under the action of an applied force. Stiffness can be represented as the slope of the idealized linear elastic curve. By equations, stiffness is the outcome of the force divided by the displacement.

$$K = V_y/\Delta_y \qquad (2.2.4)$$

Figure 1: *Elastic and Inelastic Reponses of structures.*

Figure 1a: *Overstrength factor on force-displacement curve.*

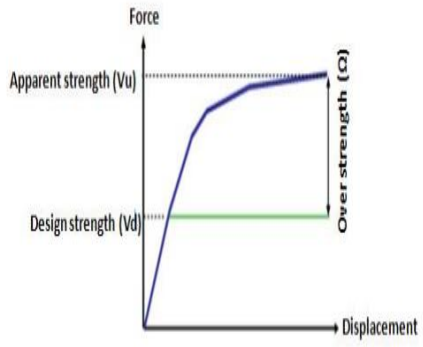

Figure 1b: *Stiffness illustration by stress-strain curve.*

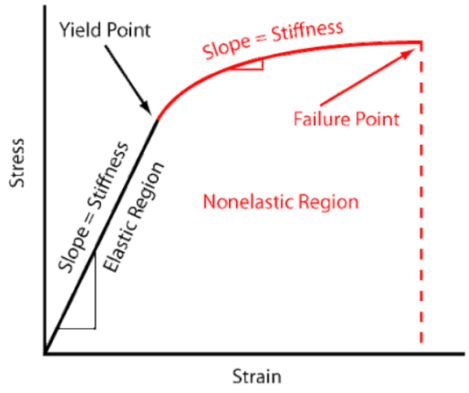

- Ductility

The ductility definition in material engineering science is the ratio of ultimate strain to yield strain of the material. In a broader view, ductility is the ability of a structure to undergo larger deformations without collapsing.

When the structure goes through a seismic demand, which can be classified as a dynamic force, the structure will no longer remain elastic, and the damage will occur. The structure also has the plastic stage, where stiffness will decrease appreciably and deformations will be drastically increasing even for a small load. To prevent the damage, ductility must be increased.

The inelastic behavior of the structure can be calculated as follows:

$$\mu = \Delta_u / \Delta_y \qquad (2.2.5)$$

Where,

μ is the displacement ductility.

Δ_u is the ultimate deformation.

Δ_y is the yielding deformation.

The relation shall be a bilinear relation, with the effective lateral stiffness K_e and effective yielding shear V_y. The location of the line segments on the force-displacement curve should be determined using an iterative graphical procedure that roughly balances the area below and above the curve.

Newmark and Hall define the response reduction factor as the ratio of maximum deformation to the yield deformation.

Newmark and hall proposed equations to determine the reduction factor ($R\mu$) as shown

$$R_\mu = 1.0 \ (T < 0.03 \text{ second}) \qquad (2.2.6)$$

$R_\mu = 2\mu - 1$ (0.12 < T < 0.03 second) (2.2.7)

$R_\mu = \mu$ (T > 1.0 second) (2.2.8)

While T. Paulay and M. J. N. Priestley sort the structure time period as following

$R_\mu = 1.0$ (zero-period structures) (2.2.9)

$R_\mu = 2\mu - 1$ (short-period structure) (2.2.10)

$R_\mu = \mu$ (long period structure) (2.2.11)

$R_\mu = 1 + (\mu - 1)\, T/0.70$ (0.70 s < T < 0.3) (2.2.12)

Also, Lai and Biggs studied the inelastic spectra for 20 artificial motions with periods equally spaced between 0.1 s and 10 s with 50 natural periods. The equation from the study is

$R_\mu = \alpha + \beta(\log T)$ (2.2.13)

In this equation, α and β represent parameters that can be found in the table located in Appendix B.

2.2.4 Response reduction factor equation

The R-factor is a significant parameter in the structural seismic design analysis by means of the non-linear response of a structure. R represents the ratio between the maximum lateral forces which would develop in the structure in the elastic case (V_e) to the lateral force (V_d) as follows:

$R = V_e/V_d$ (2.2.14)

While the ATC-19 defines the response reduction factor as the product of the strength, ductility, and redundancy factors.

R = Overstrength factor × Redundancy factor × Ductility factor

$R = Rs \times R\mu \times R_s \times R_\mu \times R_r$ (2.2.15)

However, in this study, both overstrength and redundancy are treated as components of the overstrength factor.

So, 2R = Overstrength factor × ductility reduction factor

$$R = (\Omega \times R_{\mu})/2 \quad (2.2.16)$$

2.2.5 Manual calculations

To determine the value of the response reduction factor, the ASCE code depends on the yield shear force and the equivalent lateral force.

$$R = \frac{Ve}{V} \quad (2.2.17)$$

The yield force (V_d) is the shear force that causes the reinforcement steel to yield or the concrete to start failing in shear. This point is important because it defines the point where the element stops behaving elastically and starts to behave plastically, which is critical in structural design and seismic performance.

The equivalent lateral force is calculated in accordance with the following equation:

$$V_e = C_s W \quad (2.2.18)$$

Where,

$$W = W_{dead} + W_{SID} + 0.25W_{LL} \quad (2.2.19)$$

Cs is the seismic response coefficient. The coefficient (Cs) shall be determined according to the following equation:

$$Cs = \frac{SDS}{R/I} \quad (2.2.20)$$

S_{DS} is the design spectral response acceleration in the short period range.

R is the response modification factor taken from table 9.5.2.2 in the ASCE code.

J is the occupancy importance factor

V is the yield shear force

This method was used in validation calculations.

2.3 Procedure for seismic analysis of RC Building

2.3.1 Equivalent static lateral force method by UBC-97

The design base shear shall be calculated using the following equation:

$$Vb = \frac{Cv\, I}{R\, T} W \quad (2.3.1)$$

While the base shear need not exceed the following

$$V = \frac{2.5 Ca\, I}{R} W \quad (2.3.2)$$

And shall not be less than the following

$$V = 0.11Ca \times I \times W \quad (2.3.3)$$

Where

I is the importance factor

R is the response reduction factor

C_a is the acceleration seismic factor

C_v is the velocity seismic factor

W the seismic load

The time period is determine from the equation

$$T = C_t \times h_n^{0.75} \quad (2.3.4)$$

Where,

C_t is 0.75 for the for reinforced concrete moment-resisting frames and eccentric braced steel frames

h_n is the height of the roof above the base in meters.

And the vertical distribution load is calculated by the equation

$$Fx = V_b \frac{wx\ hx}{\sum_{i=1}^{n} wi\ hi} \quad (2.3.5)$$

2.3.2 Response spectrum method

This process is used for calculating design base shear without considering the stiffness of infill.

First calculate eigenvalues and eigenvectors.

Determine mass matrices and stiffness matrices of the frame lumped mass model as

M = [M]

K = [K]

For the above stiffness and mass matrices, eigenvalues and eigenvectors are worked out as follows:

$|K-\omega^2 m|= 0$

Solving the above equation, natural frequencies (eigenvalues) of various modes can be calculated.

ωi^2 is called the "ith eigenvalue" of a matrix $[-M\ \omega i^2 +K]\ \phi i$.

Each natural frequency (ωi) of the system has a corresponding eigenvector (mode shape), which is denoted by ϕi.

The mode shape corresponding to each natural frequency is determined from the equations

$[-M\ \omega i\ 2 +K]\phi 1 =0$

$[-M\ \omega i\ 2 +K]\phi 2 =0$

$[-M\ \omega i\ 2 +K]\phi 3 =0$

$[-M\ \omega i\ 2 +K]\phi n =0$

Solving the above equations, modal vector (eigenvectors), mode shape and natural period under different modes were found

$$\{\phi\} = \{\phi 1\ \phi 2\ \phi 3\ \phi 4\text{……..}\phi n\} \quad (2.3.6)$$

The next step is the determination of modal participation factors.

The modal participation factor (Pk) of mode k shall be calculated by the equation

$$P_k = \frac{\sum_{i=}^{n} Wi\varphi ik}{\sum_{i=1}^{n} Wi(\varphi ik)^2} \quad (2.3.7)$$

Then determine the modal mass by the equation

$$M_k = \frac{[\sum_{i=1}^{n} Wi\ \varphi ik]^2}{g \sum_{i=1}^{n} Wi\ (\varphi ik)^2} \quad (2.3.8)$$

To determine the lateral force at each floor in every mode, use the following equation:

$$Q_{ik} = A_k\ \phi_{ik}\ P_k\ W_i \quad (2.3.9)$$

The peak force of a story in each mode is given by,

$$V_{ik} = \sum_{j=i+1}^{n} Qik \quad (2.3.10)$$

Determination the Story Shear Force due to all modes can be obtained as

The peak shear force (V_i) due to all modes is obtained by the square root of the sum of squares (SRSS) or the complete quadratic combination method.

If the building does not have closely spaced modes, the peak response quantity (λ) due to all modes shall be obtained as

$$\boldsymbol{\lambda} = \sqrt{\sum_{k=1}^{r} (\lambda k)^2} \quad (2.3.11)$$

2.3.3 Displacement coefficient method (FEMA-273)

FEMA-273 describes the displacement coefficient method by estimating the structural performance in terms of a target displacement representing the maximum expected displacement.

For regular structures, the pushover analysis is combined with a modified version of the equal displacement approximation related to the linear elastic spectral displacement or acceleration according to the damping and effective period of the SDOF system, and then it's corrected by the

required factors. While the irregular structure factors were examined by Karawinkler and Seneviratna.

For the DCM, a bilinear representation of the capacity curve is required. After that the effective fundamental period (T_e) is calculated as shown in the following equation

$$T_e = T_i\sqrt{Ki/Ke} \quad (2.3.12)$$

Where,

T_i is the Elastic fundamental period

K_i is the Elastic lateral stiffness of the building

K_e is the effective lateral stiffness of the building. Ke equals the secant stiffness at the base shear force equal to 60% of the effective yield strength, which is obtained from the bilinear representation of the capacity curve.

The target displacement δt in FEMA-273 is given by

$$\delta t = C_O C_1 C_2 C_3 S_a \, g \, T_e^{\,2}/4\pi^2 \quad (2.3.13)$$

Where,

C_o is a modification factor to relate spectral displacement to the structure's roof displacement, as determined by Table 3-2 of FEMA 356.

C_1 is a modification factor to relate expected maximum inelastic displacements to displacements calculated for linear elastic response as follows:

$C_1 = 1.5$ for $T_e < 0.1$ sec

$C_1 = 1.0$ for $T_e \geq T$ s

$$C_1 = [\, 1.0 + (R - 1) T_s / T_e \,] / R \text{ for } T_e < T_s \quad (2.3.14)$$

The value of C1 should not be less than 1.0.

T_s is the characteristic period of the response spectrum, defined as period associated with transition from constant acceleration segment of the spectrum to the constant velocity segment of the spectrum (to be calculated from demand spectrum)

T_e is the effective fundamental time period

$$T_e = T_i(K_i/K_e)^{1/2} \quad (2.3.15)$$

R is the ratio of elastic strength demand to calculated yield strength coefficient

$$R = S_a/(V_y/W)C_m \quad (2.3.16)$$

V_y is the effective yield strength.

S_a is the response spectrum acceleration, at the effective fundamental period and damping ratio of the building (to be calculated from demand spectrum)

C_m is the effective mass factor as determined by Table 3-1 of FEMA 356.

W is the effective seismic weight

C_2 is the modification factor used to represent the effect of pinched hysteretic shape, stiffness degradation, and strength deterioration on maximum displacement response. C_2 is taken from Table 3-3 of FEMA 356 for different framing systems and structural performance levels. Alternatively, C2 may be taken as 1.0 for a nonlinear procedure.

C_3 is the modification factor to represent increased displacement due to dynamic P-D effects

C_3= 1.0 for buildings with positive post-yield stiffness

$C3 = 1.0 + |\alpha|(R - 1)^{3/2}/T_e$ for buildings with negative post-yield stiffness (2.3.17)

α is the ratio of post-yield stiffness to effective elastic stiffness, where the non-linear force-displacement relation shall be characterized by a bilinear relation

C_0 and C_2 tables are as tabulated in the appendix

2.4 Eccentricity and Torsional Irregularity in ASCE 7-22 Compared to ASCE 7-16

Seismic design codes are developing continuously to incorporate new research and practical experiences. The American Society of Civil Engineers standard, ASCE 7, was updated from the 2016 edition (ASCE 7-16) to the 2022 edition (ASCE 7-22). This update includes important revisions related to eccentricity and torsional irregularity—two critical factors influencing the seismic parameters. This section presents a comparison between ASCE 7-16 and ASCE 7-22 provisions concerning these aspects, highlighting the main changes in the structural analysis and design.

- Treatment of Eccentricity in Seismic Design

ASCE 7-16 recommended 5% of the structural dimension as the minimum design eccentricity to account for uncertainties in mass and stiffness distribution.

Conversely, ASCE 7-22 employs detailed analytical models to ascertain the minimum eccentricity for adjustment, providing a more adaptable method. This update encourages engineers to use nonlinear static analysis to determine the effective eccentricity rather than the fixed values. This provides more optimized designs while maintaining safety, especially for torsionally sensitive structures.

- Definition and Evaluation of Torsional Irregularity

ASCE 7-16 defines torsional irregularity based on the ratio of maximum to minimum lateral displacement in the structure, with a threshold ratio of 1.2 indicating irregularity. This simplified approach may lack accuracy in complex cases.

While the ASCE 7-22 edition retains this definition but emphasizes the computational methods, recommending nonlinear or dynamic analysis to calculate torsional displacements accurately. Furthermore, ASCE 7-22 mandates consideration of bi-directional analysis effects to capture the combined influence of lateral forces in both principal directions, providing a more realistic estimation of torsional behavior.

- Impact of eccentricity and torsional irregularity on Seismic Design and Response Modification Factor (R-factor)

The Response Modification Factor (R-factor) presents the structure's ability to dissipate seismic force through inelastic behavior, thus reducing the designed elastic seismic forces. While ASCE 7-16 recognized that significant torsional irregularity could reduce the effective ductility and R-value, but it did not provide numerical adjustments.

The ASCE 7-22 clearly emphasizes the reduction in ductility and overstrength resulting from eccentricity and torsional irregularity in the structure. The code also suggests conducting detailed nonlinear analyses, including static or dynamic time-history methods, to validate the R-values. Despite the important new guidelines in the new version, there is no exact numeric reduction to the R-factor.

- Recommendations for Analysis and Design Practice

ASCE 7-22 strongly requires the use of nonlinear static (pushover) or nonlinear dynamic (time-history) analyses to capture the complex behavior under seismic loading accurately. The code also focuses on the importance of multi-directional seismic analysis for notable torsional irregularity or eccentricity cases.

The code also emphasizes the effect of accurately modeling mass distribution, including non-structural components. These recommendations aim to reduce the risk of underestimating torsional demands.

In conclusion, the updated version reflects advances in seismic research and engineering practice, enabling more accurate and realistic evaluation of eccentricity and torsional effects in the design process. By promoting detailed analysis methods effects, the updated code improves the design to predict structural response, optimize designs, and enhance safety against earthquake hazards.

2.5 Non-linear modeling of Structures

Structures that are asymmetric and have torsional irregularity require a non-linear design to achieve accurate results. Non-linear design can be implemented in Sap2000, a common structural analysis program. The non-linear response spectrum analysis is performed to design the buildings as shown in Appendix C. The modeling process involves the frame design with

suitable members and assigning plastic hinges to the maximum expected moment regions. Plastic hinges can be defined based on FEMA guidelines or inputting from specialized software that produced a moment-curvature relationship according to section properties. Nevertheless, the traditional plastic hinge model is simple; it's a limited accuracy method. To enhance the advantage of plastic hinge computational efficiency, a fiber hinge model was established. In the fiber hinge model, cross-sections are divided into many developed fibers. Thereby, the material's inelastic behavior can be captured by tracking the uniaxial stress–strain relationship of each fiber. The previous approach was based on bar-system structure mechanics and uniaxial material constitutive relationships. The mechanical response of each fiber is characterized by a uniaxial stress-strain relationship for the given material.

A beam-column element is presented in Appendix A with a fiber hinge, which is developed to track the plastic properties of each fiber's uniaxial stress-strain relationship within the cross-sections. It continues to track the development of the plastic properties of the structural members along the length of the fiber unit and the height of the section. Three aspects are requested special attention while applying a fiber hinge model: material constitutive relations, fiber hinge unit length, and cross-section division. The cross-section divisions and fiber hinge unit length are significant for computational efficiency and accuracy.

Before modeling the required case studies in Sap2000, a simple model was first established to verify the accuracy of the Sap2000 version. All necessary parameters were assigned to create the push-over curve and compare it with the standard curve.

Figure 2: *The verification model's push-over curve.*

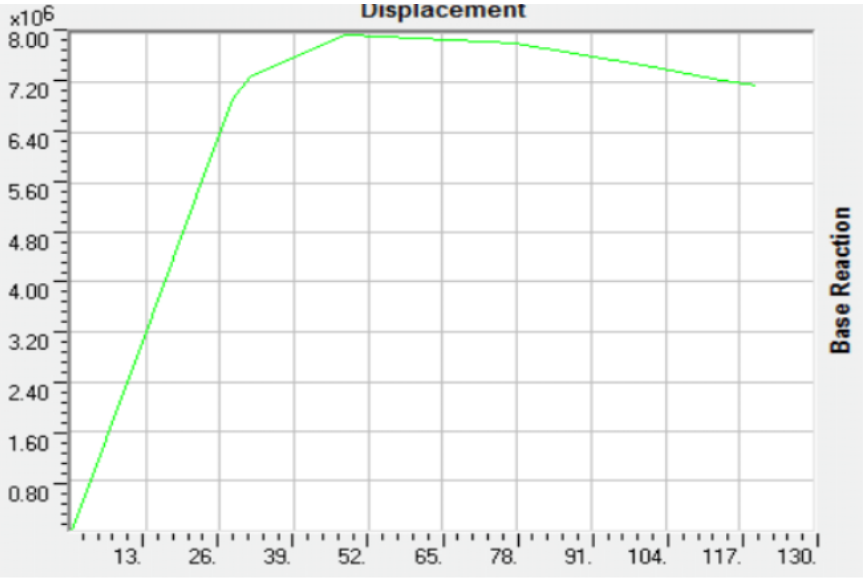

Non-Linear Modeling in SAP2000 follows the next steps

1. Design According to Code Requirements

- Ensure compliance with the ASCE code.
- Define the geometry of the structure, considering material properties (concrete and steel), cross-section dimensions, and reinforcement details for structural members based on the design standards.

2. Defining Load Cases

   Apply the structural loads, such as seismic load combinations, gravity loads, and lateral loads, as per the analysis requirements.

3. Defining Fiber Plastic Hinges

Define a suitable fiber hinge for each section by assigning fiber hinge length and section divisions to ensure a balance between accuracy and computational efficiency.

4. Running the Model and Performing Analysis

- Execute nonlinear analysis in SAP2000.

- Ensure the model requires checks.

5. Deriving P-Delta Curves

- Analyze P-Delta effects to understand geometric non-linearity behavior.
- Evaluate the influence of these effects on the structure’s overall response.

6. Tracking Plastic Hinges and Identifying Failure Modes

- Monitor the plastic hinges' behavior throughout the loading process.
- Identify the happened failure type (flexural, shear, etc.) based on hinge formation and progression.

Chapter Three
Analysis of Frames and Results

3.1 Introduction

A parametric study consisting of several models is performed to examine the effect of horizontal eccentricity on the R-factor in IMRF. In this chapter, the key parameters are identified to develop the generic model using Sap2000 program. The generic model is designed to modify and compare the R-factor results across each set of parameters. This chapter will also discuss the generic model and its characteristic parameters, aiming to achieve the research objectives.

In this chapter, the generic model is designed to systematically study the impact of horizontal eccentricity on the R-factor using essential parameters. Models are established to analyze and compare the effect of eccentricity on response reduction factors. As well, the structural characteristics, loading conditions, and analysis methods used in the study will be modified to have a comprehensive sight of the research objectives.

3.2 Characteristics of the Generic Model

A typical RC-IMRF building is designed according to the ASCE and IBC 2018 code requirements. The structures feature a square floor plan with 4-meter spans and a 3-meter story height. Different models are established with varying numbers of stories, including 5, 7, 9, 12, and 15 floors. Additionally, different eccentricity values are assigned in each model to study the paper outlines. The below figures show the 3D model of the building, the plan view, and the side view for a 5-story building with a 0.3 L structure's eccentricity indicator.

The 3D view is shown in the following figure, while the plan and side view are attached in Appendix A.

Figure 3: *3D view*

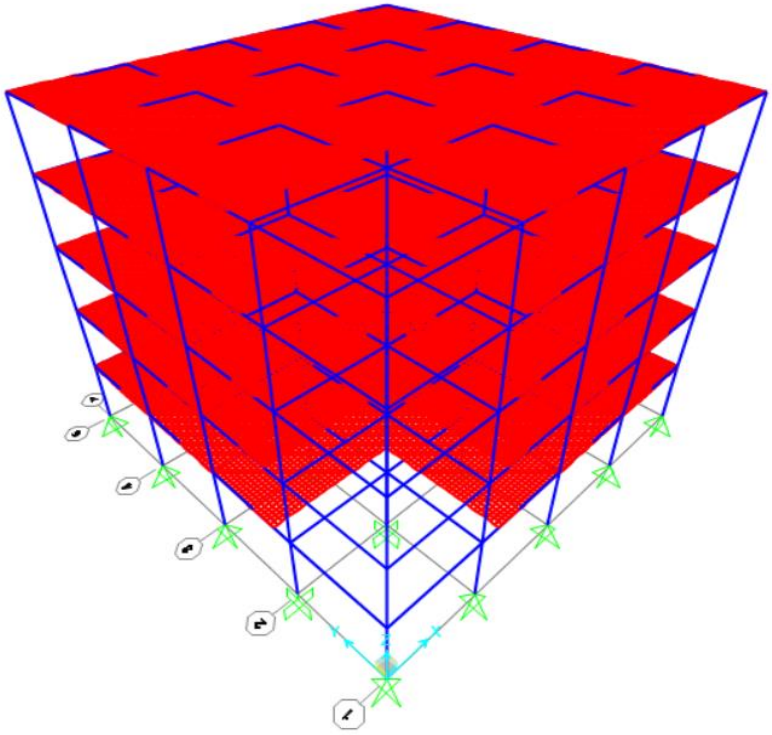

3.3 Structural system

The structure is generally designed to resist gravity loads, live loads and seismic loads. Gravity and live load are transmitted from the slabs to the foundation through the beams and columns. On the other hand, the seismic load is resisted by the structure's beams and columns.

The designed structures are IMRF systems with solid slabs, rectangular columns and beams with different dimensions according to the design requirements.

The used material properties and load combinations in Sap2000 are as mentioned in appendix C.

3.3.3 Range of Parameters

The study contains several models with different numbers of stories and eccentricity ratios using response spectrum analysis, as these are the primary parameters of interest in this research. A total of 35 cases are modeled. The buildings consisted of 5, 7, 9, 12 and 15 stories. The horizontal irregularities are varied with eccentricity indicator 0.0L, 0.1L, 0.2L, 0.3L, 0.4L, 0.5L and 0.6L. The selected values represent various cases, from a reference case with no eccentricity

to cases with horizontal eccentricity. In this study, the R-factor is compared for structures with the same height but different eccentricity ratios, and then structures with the same eccentricity value but different heights are compared. The buildings are designed following all the detailed requirements of the ACI code. However, the constant geometrical configurations for all models are illustrated below.

The eccentricity indicator is defined based on the size of the story opening in the structure. Eccentricity is introduced by creating a square opening whose side length varies from 0L to 0.6L with an increment of 0.1L relative to the story length. Therefore, the studied relationship is between the eccentricity indicator and the response reduction factor (R-factor). The eccentricity for each case was calculated based on the eccentricity indicator using the adopted calculation equation, and the resulting eccentricity values for all cases are presented as explained in the following section.

The number of spans in the x-direction is 4.
The number of spans in the y-direction is 4.
Span length in each direction is 4 m.
Slab thickness is 25 cm.
The beam's dimensions are 30×30 cm with top reinforcement of 3Ø12 and bottom reinforcement of 2Ø10.

3.3.4 Case study calculations

Since the study includes 35 models to examine the impact of torsional irregularity on R-value, a 5-story structure with an eccentricity indicator of 0.3L was selected as the case study, as it represents the key variations influencing the structural response. The model was designed as an IMRF system using nonlinear analysis in SAP2000.

As mentioned, the selected case study is a 5-story square structure with plan dimensions of 16 m × 16 m with a 0.3 L eccentricity indicator. The building columns are decreasing in size with height to reach more economical efficiency. The structural details are as follows:

- Plan dimensions: 16m × 16m
- Number of stories: 5

- Structural system: Intermediate Moment Resisting Frame (IMRF)
- Seismic analysis type: Non-linear pushover analysis (SAP2000)
- The concrete is M-24 grade with fc 28 Mpa.
- The steel is ASTM Grade 60 with fy 420 Mpa.
- The eccentricity indicator length in each direction is 4.8 (0.3L).
- Slab thickness is 25 cm.
- The beam's dimensions are 30×30 cm with top reinforcement of 3Ø12 and bottom reinforcement of 2Ø10.
- Column dimensions and reinforcement (Table 6):

Table 1: *Column dimensions.*

Story Number	Column Width (cm)	Column Depth (cm)	Reinforcement
1st & 2nd	30	30	8Ø12
3rd & 4th	25	25	4014
5th	25	25	4014

To introduce torsional irregularity, the case study eccentricity is 0.3L in both directions

- Mass center

Mass center in the x-direction (CMx) = 16/2 = 8 m.
Mass center in the y-direction (CMy) = 16/2 = 8 m.

- Stiffness center

The stiffness mass in the x-direction is CRx = CMx − e = 8 − 4.8 = 3.2 m.
The stiffness mass in the y-direction is Cry = CMy – e = 8 − 4.8 = 3.2 m.

- The eccentricity according to holes

$A_{net} = A_{total} - A_{hole}$ (3.3.1)

$x' = \frac{(Atotal \times center) - (Ahole \times hole\ center)}{Anet}$ (3.3.2)

$\Delta x = x - x'$

$e_{total} = \sqrt{\Delta x^2 + \Delta y^2}$ (3.3.3)

when the hole is 0.3 L with dimensions 0.48 m × 0.48 m

A_{net} = (16×16)-(4.8×4.8) = 232.96 m²

$x' = \frac{(256\times8)-(23.04\times2.4)}{232.96}$ = 8.55 m

Δx = 8.55 - 8 = 0.55 m = Δy

$e_{total} = \sqrt{0.55^2 + 0.55^2}$ = 0.55m

In the same progress for eccentricity indicator ratios 0L, 0.1L, 0.2L, 0.3L, 0.4L, 0.5L and 0.6L, the eccentricities are 0, 0.07, 0.27, 0.56, 0.91, 1.33, and 1.8 m.

The case study checks were done as follows:

- ***Compatibility check***

The compatibility check is done to ensure that all members are connected to each other. The check is Ok for all cases. The case study check is attached in Appendix A.

- ***Equilibrium check***

The hand-calculated loads must compare with the Sap results

- The dead load hand calculations is done as the next equation

Weight = Area × Height × Unit weight ×Members number × Story numbers

Slab weight = 233 × 0.15 × 25 × 1 × 5 = 4368.75 kN

Columns weight (0.3×0.3) = 0.3 × 0.3 × 3 × 25 × 25 × 2 = 337.5 kN

Columns weight (0.25×0.25) = 0.25 × 0.25 × 3 × 25 × 25 × 3 = 351.6 kN

Beams weight (0.25×0.25) = 0.25 × 0.25 × 4 × 25 × 20 × 5 =625 kN

- Live load and superimposed dead load hand calculations.

Weight = Area × Load ×Number of stories

Live load weight = 233 × 3 × 5 = 3495 kN
Super-imposed dead load weight = 233 × 4 × 5 = 4660 kN

Table 2: *The equilibrium check calculations.*

The load	Hand calculations	Sap2000 Result	Acceptance
Dead load	5,682.85	5559.125	Ok (Less than 5%)
Live Load	3495	3495	Ok
Superimposed load	4660	4660	Ok

- ***Drift check***

As mentioned before, the torsional irregularity is the ratio of the maximum story drift to the average story drifts. The ASCE code defines the structure as a torsional irregularity case when the ratio is larger than 1.2. On the other hand, extreme torsional irregularity occurs when the maximum story drift at one end of the structure transverse to an axis is more than 1.4 times the average of the story drifts at the two ends of the structure.

Torsional irregularity was presented in this study by removing regular parts from the slab to change the structural stiffness. The asymmetric plan could change the structure's center, which causes torsional irregularity.

In this study, a torsional irregularity case is needed to study its effect on the response reduction factor. So, for each case, the torsional irregularity was checked.

The drift check was performed for all models to ensure the structures are within the required range. The check was done according to the ASCE code. A sample table for the 5-story building is shown in Table 3, while others are tabulated in Appendix C.

Table 3: *The torsional irregularity check for 5-story building with eccentricity indicator of 0.3L*

Story number	Max drift	Average drift	Ratio
Story 5	18.84	15.71	1.199
Story 4	21.86	18.1	1.21
Story 3	29.1	24.18	1.2
Story 2	33	27.23	1.21
Story 1	64.71	54.2	1.194

3.3.5 Seismic load definition

Seismic load definition requires having the seismic parameters according to the zone properties. Response spectrum analysis is used to accommodate the seismic forces. However, equivalent static analysis is used to obtain the theoretical input values and for comparison with the response

spectrum according to the code requirements. The calculations have been done using ASCE code tables and equations.

- Risk category = II
- The value can be taken from the seismic hazard map in Palestine in Appendix A.

The study was done in zone 2B, and therefore Z=0.2, as attached in Appendix A.

- Spectral acceleration

$S_s = 2.5 \times 1.5 \times Z$

$S_s = 2.5 \times 1.5 \times 0.2$

$S_s = 0.75$

$S_1 = 1.5 \times 1.25 \times Z$

$S_1 = 1.5 \times 1.25 \times 0.2$

$S_1 = 0.375$

- Site classification

To determine the site class, soil strength is required. The ASCE table in Appendix B describes the values.

q_{all} is 150 kN/m^2

Site class is C

The soil classification used in this study is class C. According to the ACSE-07-16 code, the redundancy factor in this case is 1.0, as shown in Appendix A.

- Long- and short-period site coefficients

Short-period site coefficient (Fa)

From table 11.4-1 in the ASCE code with a site class C and Ss = 0.75, the short-period coefficient Fa is 1.1.

Long-period site coefficient (Fv)

From table 11.4-2 in the ASCE code with a site class C and S_1 = 0.375, the long-period coefficient Fv is 1.475.

- Design spectral acceleration

$SD_s = \frac{2}{3} \times Fa \times Ss.$

$SD_s = \frac{2}{3} \times 1.1 \times 0.75$

$SD_s = 0.55$

$SD_1 = \frac{2}{3} \times Fv \times S_1$

$SD_1 = \frac{2}{3} \times 1.475 \times 0.375$

$SD_1 = 0.36875 \cong 0.37$

- Seismic design category

From table 9.5.2.2 of the ASCE code, design spectral acceleration values (SDs=0.55 and SD_1=0.37, and a risk category is II the seismic design category is C.

- Structural system coefficient

The structural system used is the intermediate moment-resisting frame (IMRF).

The coefficients can be determined from the same table as follows:

Response modification coefficient (R) is 5

The overstrength factor (Ω) is 3

The deflection amplification factor (Cd) is 4.5

The analysis procedure used is the equivalent lateral force procedure. The analysis was checked by table 12.6-1.

3.3.6 Pushover load definition

For the pushover analysis, the gravity loads have to be defined as a nonlinear case before the lateral load starts acting on the structure. As the IBC code mentioned, the nonlinear gravity load must contain the full dead load capacity and 25% of the live load.

After the nonlinear gravity load definition, the pushover loads in the X-direction and in the Y-direction were added.

3.3.7 Code requirements for extreme torsional irregularity.

The effect of additional demand by 25% on seismic load for extreme torsional irregularity on the structure is applied to these cases. The extreme cases with different numbers of stories were redesigned considering additional demands of 25%. No change is documented in the elements' design, and consequently, no significant change is observed in the push-over curves as shown in appendix C.

3.4 Analysis and interpretation of results

3.4.1 Models creation

In this research, 35 models were designed to study the effect of having eccentricity in the structure on the R-factor for IMRF structures. The main parameters are the structure’s height (number of floors) and the eccentricity ratio. A pushover analysis was considered for each case to create the load-deformation curves, which were subsequently used to calculate R-factor values.

The R-factor value for the uniform IMRS structure is 5, as specified in the ASCE 7-16 code. Therefore, a comparison between the code value and the calculated R-factor will be executed.

3.4.2 Natural period of the structures

The natural period for the models were taken from the Sap2000 then checked by the code equation

$$T = 0.075 \times h^{0.75} \quad (3.4.1)$$

The results of the natural period from Sap2000 and code equation were summarized in the table

Table 4: *Natural period values for each case of the study.*

No stories	eccentricity indicator ratio	T (Sap)	T (code)	No stories	eccentricity indicator ratio	T (Sap)	T (code)
5	0	0.6	0.57	9	0.4	0.98	0.89
5	0.1	0.63	0.57	9	0.5	0.97	0.89
5	0.2	0.62	0.57	9	0.6	0.95	0.89
5	0.3	0.62	0.57	12	0	1.2	1.1
5	0.4	0.61	0.57	12	0.1	1.2	1.1
5	0.5	0.6	0.57	12	0.2	1.2	1.1
5	0.6	0.58	0.57	12	0.3	1.2	1.1
7	0	0.8	0.74	12	0.4	1.2	1.1
7	0.1	0.8	0.74	12	0.5	1.18	1.1
7	0.2	0.79	0.74	12	0.6	1.19	1.1
7	0.3	0.79	0.74	15	0	1.4	1.3
7	0.4	0.77	0.74	15	0.1	1.4	1.3
7	0.5	0.76	0.74	15	0.2	1.4	1.3
7	0.6	0.75	0.74	15	0.3	1.4	1.3
9	0	1	0.89	15	0.4	1.4	1.3
9	0.1	1	0.89	15	0.5	1.4	1.3
9	0.2	1	0.89	15	0.6	1.4	1.3
9	0.3	1	0.89				

3.4.3 Static pushover curves

As shown in the previous sections, the pushover analyses were done using Sap2000 program to calculate R-factor values. In this section, the static pushover curves for each model will be presented to assess the effect of the eccentricity ratio on the structure pushover curve.

The following figures clarified the differences between the pushover curves for models with the same number of stories but varying eccentricity ratios for each case. This step will highlight the influence of eccentricity changes on the structure's performance.

Figure 4: *Static pushover curves for the models.*

Figure 4-a: *5-story push-over curves.*

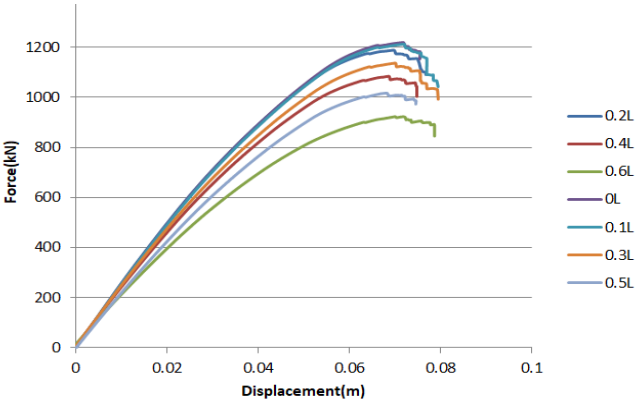

Figure 4-b: *7-story push-over curves.*

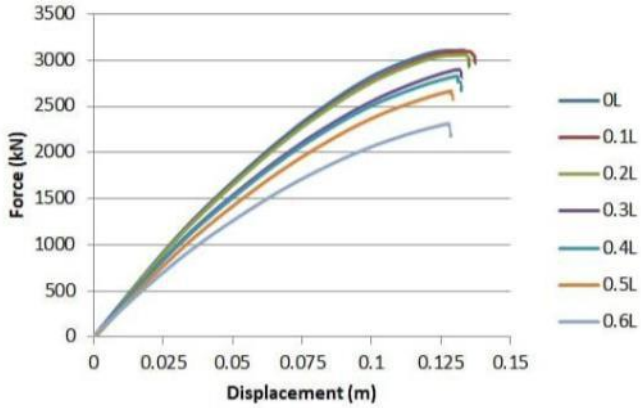

Figure 4-c*: 9-story push-over curves.*

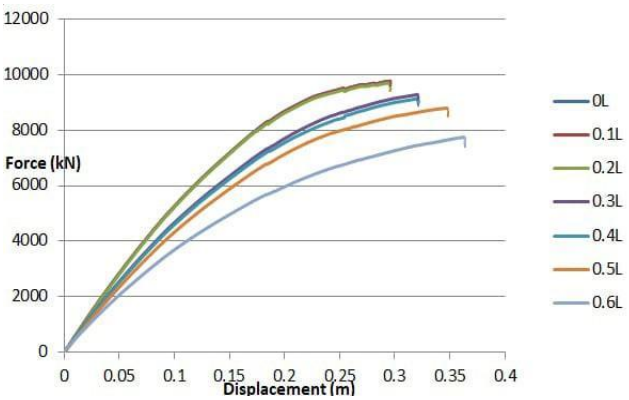

Figure 4-d: *12-story push-over curves.*

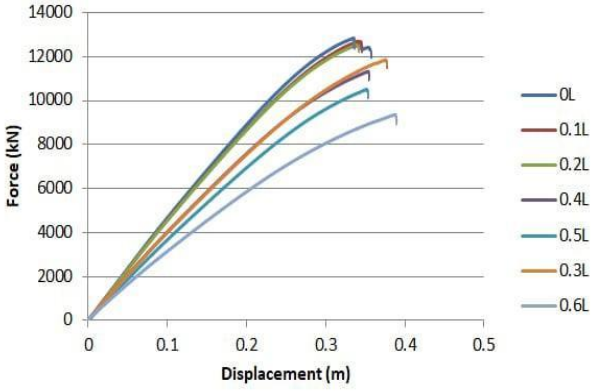

Figure 4-e: *15-story push-over curves.*

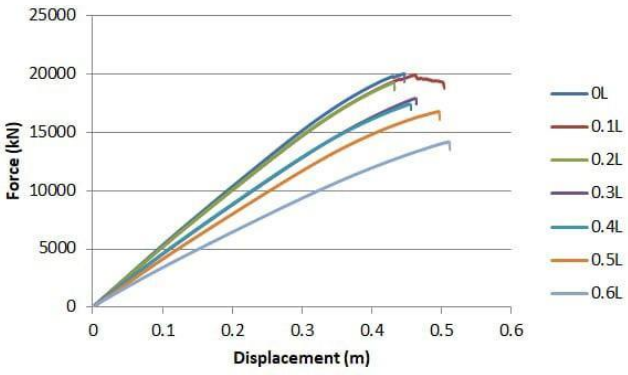

The decrease in the ductility and durability of the structure when increasing the eccentricity indicator dimensions as the eccentricity also increases is clear according to the previous figures.

3.4.4 Response reduction factor calculation

As mentioned before, the calculations will be done according to the code equation

$$R = V_e/V \quad (3.4.1).$$

Where,

V_e is the equivalent shear force.

V is the yield shear force. The yield force is the lateral force corresponding to the point where the structure transitions from the initial elastic range to the inelastic range. This yield point is determined by idealizing the original pushover curve into a bilinear curve such that the area under the initial linear portion of the bilinear curve approximately equals the elastic energy stored in the original curve. The yield force represents the maximum force that the structure can resist while still behaving elastically, beyond which plastic deformations start to develop. This value is a key parameter for evaluating the seismic performance and ductility of the structure. The point detect from the bilinear approximation figure as an example for 15-story with a 0.6L eccentricity indicator ratio.

Figure 5: *bilinear approximation for 15 stories with eccentricity indicator of 0.6L.*

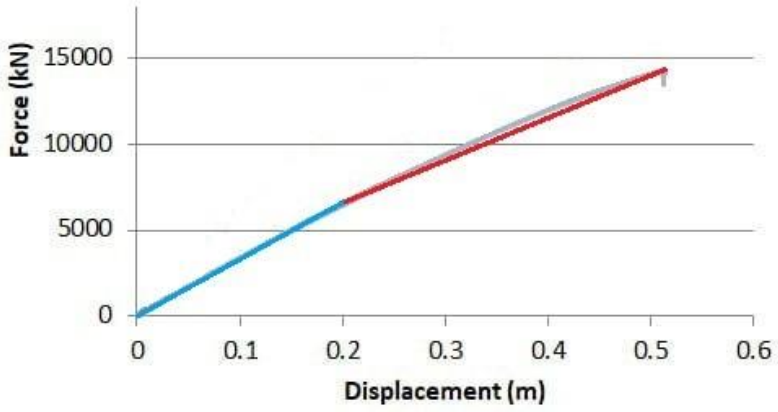

After defining the structure's elements on Sap2000 program, the program did all the required analysis to get the accurate results. Therefore, the program can provide all necessary information, including the structure's weight and the yield shear force.

In the section's case study, the results were as follows:

W_{Dead} is 6321.1 kN

W_{SID} is 4660 kN

W_{Live} is 3495 kN

So the Ve is 4721.8 kN

V is 976 kN

From the previous information R = 4721.8/976

R = 4.838

Continue the calculations as explained for all the models; the results appear as follows.

Table 5: *R-factor calculation's results.*

No stories	eccentricity indicator ratio	W_{dead} (kN)	W_{SID} (kN)	W_{Live}(kN)	V_e (kN)	V (kN)	R
5	0	6759	5120	3840	5107.97	1032	4.95
5	0.1	6717	5075	3806	5070.56	1021	4.96
5	0.2	6633	4915	3687	4965.64	1013	4.9
5	0.3	6321	4660	3495	4721.875	976	4.83
5	0.4	6007	4301	3226	4432.458	931	4.76
5	0.5	5559	3840	2880	4041.624	892	4.53
5	0.6	5007	3277	2458	3562.138	803	4.43
7	0	9926	7168	5376	11062.76	2203	5.022
7	0.1	9859	7096	5322	10971.38	2196	4.996
7	0.2	9657	6881	5161	10697.19	2187	4.891
7	0.3	9254	6523	4892	10199.91	2135	4.777
7	0.4	8851	6021	4516	9600.49	2097	4.578
7	0.5	8246	5376	4032	8777.962	1974	4.447
7	0.6	7507	4588	3441	7772.651	1801	4.316
9	0	17778	9216	6912	17233.09	3573	4.82
9	0.1	17663	9124	6843	17067.2	3568	4.78
9	0.2	17317	8847	6636	16642.11	3563	4.67
9	0.3	16741	8387	6290	15947.46	3417	4.67
9	0.4	16024	7741	5806	15036.99	3299	4.56
9	0.5	14898	6912	5184	13749.44	3178	4.33
9	0.6	13631	5898	4424	11717.31	2855	4.10

12	0	28828	12288	9216	26052.08	5302	4.91
12	0.1	28636	12165	9124	25807.85	5276	4.89
12	0.2	28052	11796	8847	25167	5191	4.85
12	0.3	27100	11182	8387	24130.54	5091	4.74
12	0.4	25756	10322	7741	22683.63	5151	4.40
12	0.5	24028	9216	6912	20831.21	4824	4.32
12	0.6	21916	7864	5898	17868.27	4303	4.15
15	0	41564	15360	11520	35882.44	7538	4.76
15	0.1	41276	15206	11405	35548.36	7488	4.75
15	0.2	40417	14746	11059	34669.96	7426	4.67
15	0.3	38972	13978	10483	33221.32	7387	4.50
15	0.4	36966	12902	9677	31216.84	7302	4.28
15	0.5	34364	11520	8640	28636.36	6982	4.10
15	0.6	31254	9830	7373	24650.44	6613	3.73

3.4.5 Effect of considering combined flexural/shear/torsional hinges

The thesis adopted this point as one of its main assumptions. However, the thesis addresses other scenarios by incorporating shear and torsion plastic hinges in series with the flexural plastic hinge in every column. Shear hinges were added to the structural modeling to represent the inelastic shear behavior of columns and capture the shear deformation and strength degradation that occur after cracking and yielding. The shear hinges were applied manually in SAP2000 at the two ends of the columns. The application followed the guidelines of ASCE 41-17, which specifies the hinge locations and parameters for nonlinear modeling. In SAP2000, the hinge was defined using the shear hinge type and the plastic hinge properties were selected from the program's built-in ASCE 41 hinge library.

Torsion hinges are used to simulate the inelastic torsional behavior in structures when subjected to twisting due to eccentricity or irregular geometry in buildings. The importance of torsional

hinges is to capture the redistribution of torsional moments and the possible stiffness degradation that happened from cracking or yielding in the structure. Torsion hinges were also added to each top and bottom of the columns. The torsion hinge type is a moment-rotation isotropic hinge with immediate occupancy of 0.003, life safety of 0.012, and collapse prevention of 0.015. Based on ASCE 41-17, the allowable torsional rotations ranged from 0.002 rad for elastic behavior up to 0.03 rad at collapse.

This consideration causes a minor change in force, a considerable change in ultimate deformation, and consequently a change in the R-factor, as shown in Table 6. This point is performed on the cases of extreme torsional irregularity as shown in the figure in Appendix C. The change in R-values before and after adding the additional hinges was approximately 5%, whereas when comparing this result to the code R-value, the change ranged from 15% to 30%, as shown in Table 8. Additionally, V/M ratios for cases with zero irregularity and the corresponding ratios for the cases with different values of irregularities are tabulated in Appendix C for the critical column. This shows that effect of irregularity has minimal effect on V/M ratio, as V/M is approximately constant for buildings with the same height, as shown in figure 6.

Figure 6: *Comparison between push-over curves before and after adding the shear-tension hinges for the same structure.*

Figure 6-a: *5 stories structure comparison.*

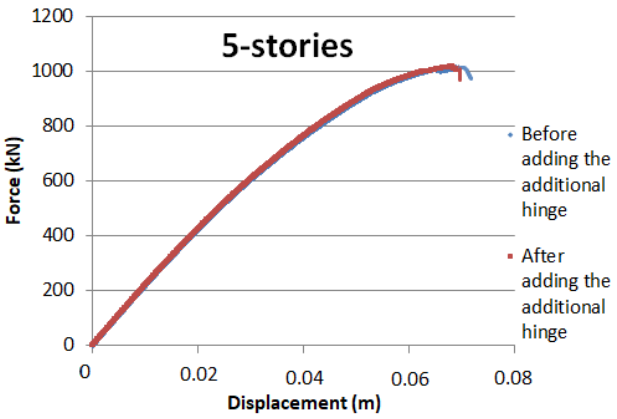

Figure 6-b: *15-stories structure comparison.*

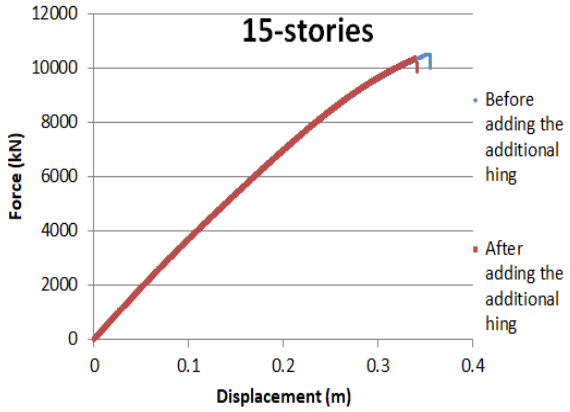

3.4.6 The decrease in R-factor

To recapitulate the effect of the R-factor, the tables below describe the reduction percentage in R-factor for each case. Each table presents a specific number of floors along with their

corresponding eccentricity ratios. The table compares the value of the R-factor without eccentricity with the R-factor with eccentricity

Table 6: *The reduction percentage of the R-factor for each structure.*

No stories	eccentricity indicator ratio	R reduction%	No stories	eccentricity indicator ratio	R reduction%
5	0	0	9	0.4	5.4
5	0.1	0.3	9	0.5	10.2
5	0.2	1.0	9	0.6	14.9
5	0.3	2.3	12	0	0
5	0.4	3.8	12	0.1	0.4
5	0.5	8.5	12	0.2	1.3
5	0.6	10.4	12	0.3	3.5
5*	0.6	15.2	12	0.4	10.3
7	0	0	12	0.5	12.1
7	0.1	0.5	12	0.6	15.4
7	0.2	2.2	15	0	0
7	0.3	3.8	15	0.1	0.3
7	0.4	8.4	15	0.2	1.9
7	0.5	11	15	0.3	5.5
7	0.6	13.68	15	0.4	10.2
9	0	0	15	0.5	13.8
9	0.1	0.8	15	0.6	21.7
9	0.2	3.1	15	0.6	21.7
9	0.3	3.1	15*	0.6	29.8

Note: The * present the cases with combined flexural/shear/torsion hinge cases

The previous calculations demonstrate the observed impact of eccentricity on seismic design overall and specifically on the R-factor. For the 5-story structures, the R-factor decreased about 10% when moving from a uniform plan to a 0.6L eccentricity plan. The 7-, 9-, and 12-story structures experience a reduction of approximately 15%. While in the 15-story structure, the ratio increases to reach 22%.

The reduction percentage can be described as the charts shown.

Figure 7: *illustrates the relationship between eccentricity and the R-factor reduction percentage for each story number.*

Figure 7-a: *The R-factor reduction percentage according to the eccentricity indicator ratio as curves.*

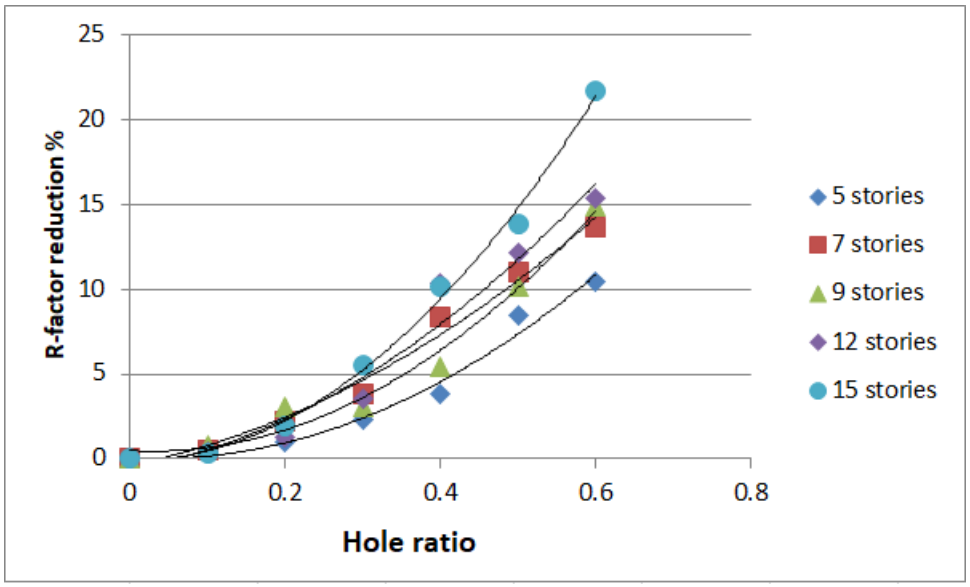

Figure 7-b: *The R-factor reduction percentage is represented as bars based on the eccentricity indicator ratio.*

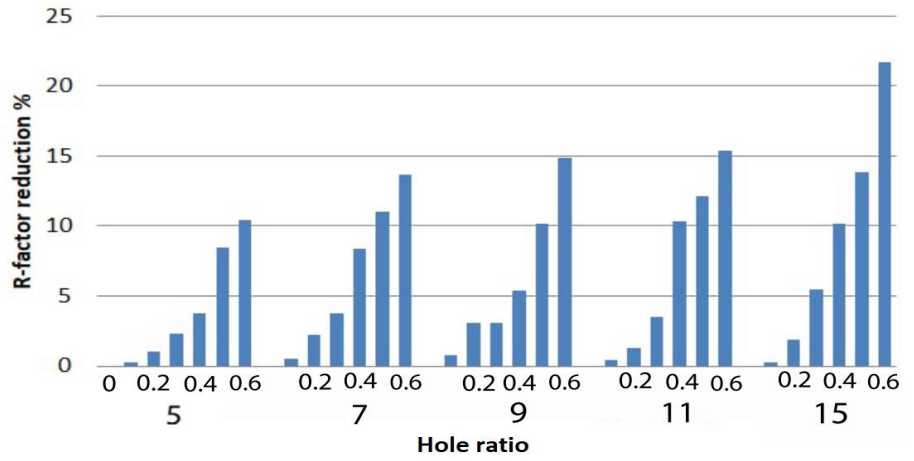

3.4.7 Eccentric Bi-Directional Load Effect

In pushover analysis, base shear and displacement normalization are applied to enable comparison between different structural configurations regardless of their absolute strength or stiffness. This is achieved by scaling the response parameters with respect to reference values, such as yield displacement and maximum base shear in the model.

In structures with torsional irregularity, the presence of eccentricity between the mass center (CM) and the rigidity center (CR) causes seismic loading to have a coupled bi-directional nature. When lateral seismic forces act, the eccentricity generates a torque, as the equation shows, producing simultaneous translational and rotational responses.

$$M_t = F_{lat} \times e \tag{3.4.1}$$

In other words, when the structural response is not purely translational, a bi-dimensional coupling between lateral displacements and rotational components around the vertical axis is involved. In such cases, the torque generated from eccentricity redistributes the lateral forces between frames in orthogonal directions. This results in a non-uniform lateral stiffness and an asymmetric distribution of plastic hinges in the structure.

Pushover curve normalization involves dividing the displacement values of different models by the maximum displacement of the structure, allowing for a comparison based on relative behavior rather than absolute values while also considering the bidirectional effects of seismic forces. This process removes scale bias and highlights the relative performance of the structures, particularly in terms of stiffness degradation, ductility, and failure mechanisms. By converting the data into a common scale, normalization enhances the clarity of visual interpretation and supports more generalized conclusions about the influence of torsional irregularity and increased seismic force demand.

Normalization was applied to clarify the bi-directional effect on the push-over curve results. The comparison was done on the 15-story model with a 0.6 L eccentricity indicator ratio in order to check the pushover curve before and after normalization. The displacement at each corner of every story was extracted and then divided by the maximum displacement value. The total base shear was redistributed as joint loads at each corner point to allow the model to be reanalyzed.

A notable effect is observed in the nonlinear part of the pushover curve, while a negligible contribution is noted in the elastic range. The joint loads on each corner led to a more realistic distribution of joint loads during the pushover analysis. The post-normalization curve became more representative of the actual behavior of the structure. The normalized model captured the effect of eccentricity more clearly and provided a more profound understanding of how irregularity influences the distribution of deformation and the progression of damage. The R-value was also affected and became 3.61 instead of 3.73. An additional reduction of R-value by 3.2% is recorded. The pushover curves before and after the bi-dimensional process is shown in Figure 8.

Figure 8: *The effect of bi-dimensional process on the push-over curve.*

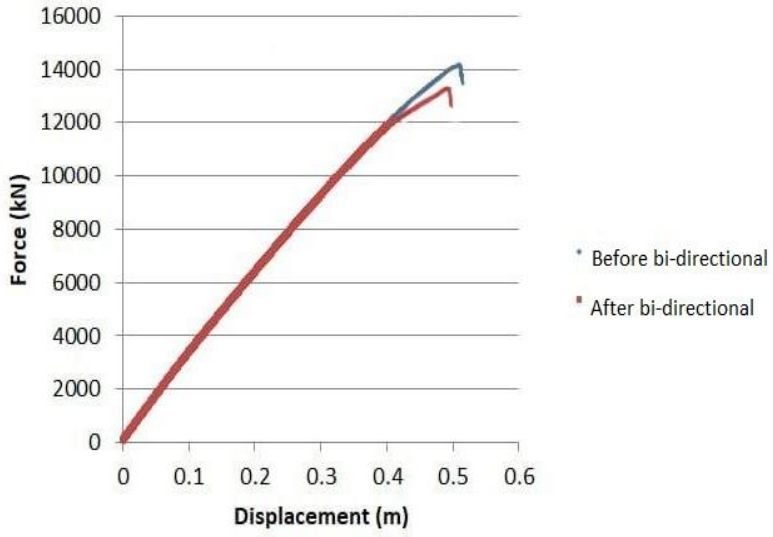

3.4.8 Structure failure mechanism

Structural failure refers to the inability of a load-bearing component of a building to support and transfer loads to another element. Structural failure develops due to a breakdown in the performance of the materials in a structural component.

A “failure” does not necessarily refer to the immediate or sudden collapse of the structure. Excess loads can also slowly diminish structural integrity over time. This persistent stress gradually weakens the structure until it cans no longer stand, at which point a collapse occurs (Maggiano, DiGirolamo & Lizzi)

In some cases, the structural load-bearing component becomes unable to support and transfer loads to another element, which leads to a structural failure in the building. As the performance of materials breaks down, the structural failure will develop.

The breakdown of materials may occur for the following reasons:

- Foundation failure: The foundation is established to carry the loads from the structure to the ground; when a foundation failure occurs, a defect in the load-carrying process has happened.
- Overloading occurs when an unexpected load, not accounted for in the design analysis, imposes excess loads on the structure, potentially leading to structural failure. The excess loads could be from an earthquake, change of use, or hurricanes.
- Improper design: any design fault may lead the structure to a horrible case of construction failure. The design analysis is a very accurate process; the designer has to pay attention to every single detail of the construction.
- Erroneous construction: another critical factor, inaccurate construction as a result of the engineer supervising the construction activities or faults in the construction elements.

The construction failure has different types, such as

- Compressive failure

  Sudden catastrophic phenomenon apparent by cross breaks caused by the excessive longitudinal compression or bending in the structure.

- Tensile failure.

  The failure caused by the tension force manifests as cracks that are perpendicular to the direction of the tensile force. The failure is detected by the stretching of the members.
- Bending failure

  Bending failure, also known as flexural stress, occurs when an object is subjected to external forces that cause bending or deformation in the subject.
- Buckling failure

  Buckling occurs when the load reaches the critical load due to the axial load applied to the member's longitudinal axis.

Although buckling occurs abruptly, the structural members typically do not fracture. When buckling happens in a member, it causes instability; excessive stresses occur in the whole structure, which may lead to a progressive collapse.

In the irregular structure, the difference between the mass center and the rigidity center causes torsional moment around the center of rigidity, which creates additional shear on the building's columns. The massive amount of shear force on the columns, in addition to the earthquake force affecting the structure, causes partial structural damage or total collapse.

In the case studies, the main effective parameter, as mentioned before, is the torsional irregularity in the structures. Referring back to the pushover curves, sudden collapses are clearly observed in some structures, which leads to an unexpected decrease in shear forces. When a structural element undergoes large deformation, it is assumed that the deformation affects a point called a plastic hinge. The force deformation behavior of the plastic hinge can be defined in five points: A, B, C, D and E, where A is the origin point, B is the yielding point, C describes the ultimate point, and D and E are the residual strength and displacement capacity. Another three points can be labeled to define the acceptance criteria for the plastic hinge, as in FEMA and ATC 40, as shown in the figure in Appendix A.

IO is the immediate occupancy, which refers to light overall damage in the building. LS is the life safety stage, which indicates significant structural and nonstructural damage, as well as a loss of structural stiffness and strength. CP is the collapse prevention; the CP level occurs when the building loses most of its stiffness and strength, so the building is near to collapse.

After the previous collapse criteria and information, the studies immediate collapse reasons are clear. The required IO, LS, and CP points for each structure were taken and assigned in the table.

As described in figure 9-a, a row of columns in the structure reaches the failure stage, which causes an error in the load transfer category. Thereby, a structural failure occurs immediately while the other columns are in the yielding stage due to the eccentricity in the structure. And figure 9-b shows the difference between the columns located in a torsional irregularity structure. Some columns are in the collapse area, while others with lower loads are still in the yielding area. Figure 10 compares the cases with the same story number but different eccentricity ratios.

Table 7: *Plastic hinge stages of the structures.*

NO. stories	eccentricity indicator ratio	IO force (kN)	LS force (kN)	CP force (kN)	NO. stories	eccentricity indicator ratio	IO force (kN)	LS force (kN)	CP force (kN)
5	0	936	1081	1206	9	0.4	1703	5927	7601
5	0.1	928	1072	1197	9	0.5	1624	5578	7215
5	0.2	955	1069	1179	9	0.6	1468	4714	6083
5	0.3	953	1058	1055	12	0	2254	7000	11651
5	0.4	869	1056	1011	12	0.1	2194	6830	11318
5	0.5	828	1008	994	12	0.2	2170	6803	11055
5	0.6	806	921	892	12	0.3	2022	5910	9509
7	0	1047	2927	3109	12	0.4	1916	5920	9476
7	0.1	1229	2889	3095	12	0.5	1614	5358	8912
7	0.2	1162	2801	3048	12	0.6	1302	5023	8063
7	0.3	1127	2798	2901	15	0	3037	11959	17237
7	0.4	1084	2575	2829	15	0.1	2943	11564	16728
7	0.5	1006	2461	2667	15	0.2	2900	11605	16744
7	0.6	873	2127	2314	15	0.3	2547	9422	13837
9	0	2057	6612	8621	15	0.4	2579	9369	13860
9	0.1	2017	6524	8473	15	0.5	2501	9400	13030
9	0.2	2026	6457	8590	15	0.6	2039	7484	12744
9	0.3	1807	6012	7733					

Figure 9: *Column failure.*

Figure 9-a: *Front view for the case study failure*

Figure 9-b: *Side view for the case study failure*

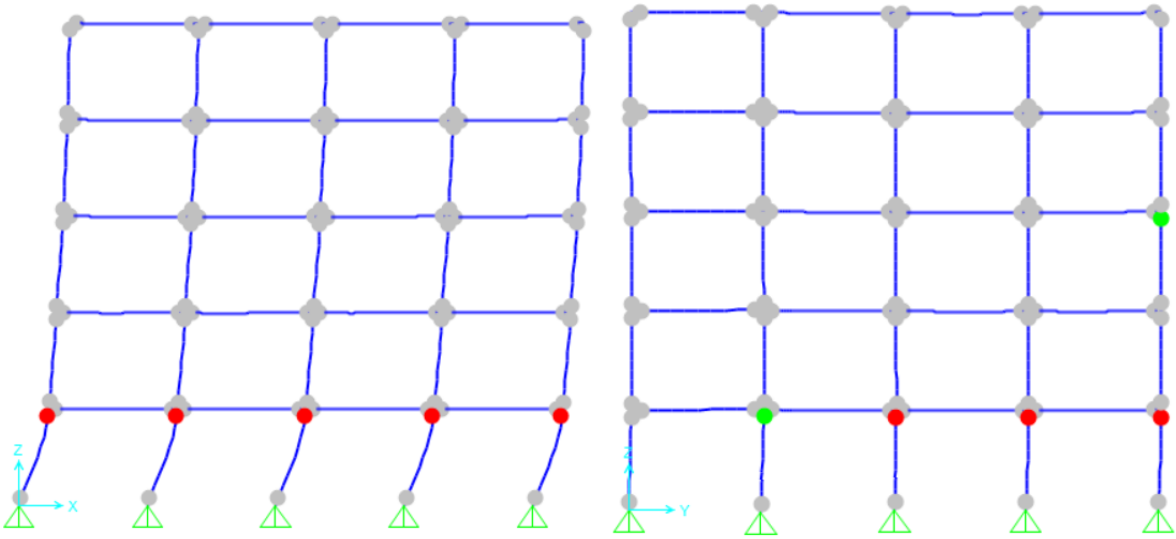

Figure 10: *Comparison between various eccentricity ratios for 5-stories.*

Figure 10-a: e- indicator=0

Figure 10-b: *e-indicator=0.3L*

Figure 10-c: *e-indicator=0.6L*

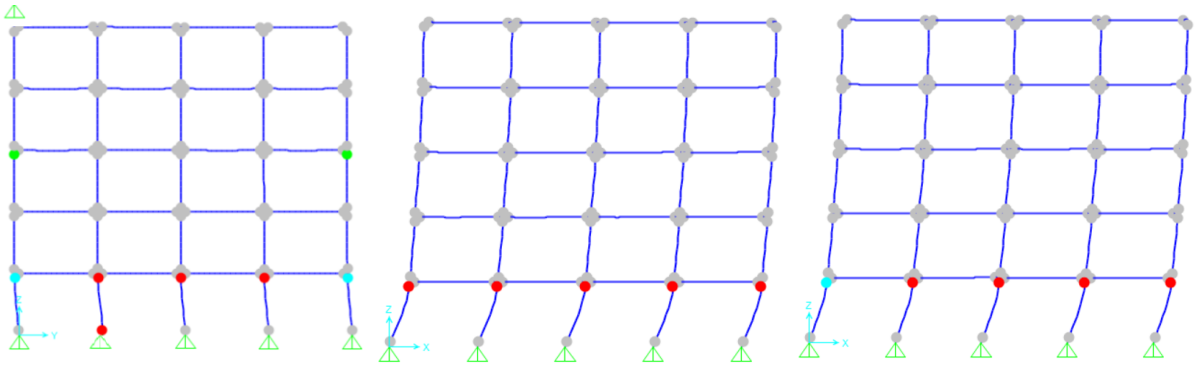

Chapter four

Conclusion and future work

4.1 Summary

This thesis examined the change of the response reduction factor (R-factor) for a reinforced concrete Intermediate Moment Resisting Frame (IMRF) with an asymmetric layout. The design method and computations adhered to the ASCE 7-16 standard. The prescribed R-factor values from the code were juxtaposed with the values from each engineered model. Various models were constructed and examined through push-over analysis utilizing SAP2000 commercial software to investigate the impact of horizontal eccentricity on the R-factor of the building. The initial set of models featured differing numbers of stories with a consistent eccentricity ratio, but the subsequent set was constructed with varying eccentricity ratios with a uniform number of stories. The load-deflection curves were utilized to compute R-factor values for comparison purposes. Various forms of push-over curves were utilized to examine distinct loading scenarios and plastic hinge formations. A minor variation is observed between these examples. The principal findings of the study are reported in the subsequent section.

4.2 Conclusions

The American standards document a constant value of the R-factor of "five" for IMRF. However, this study shows a reduction of R-factor for the cases with a high level of horizontal eccentricity, "horizontal irregularity," especially for tall buildings. The goal of this study is to investigate the Response Reduction Factor (R-factor) for reinforced concrete Intermediate Moment Resisting Frames (RC-IMRFs) with asymmetric plans when there is a difference between mass and stiffness centers in seismic design according to the ASCE 7-16 design code. The findings of the study clarify the accurate effect of horizontal eccentricity on the R-factor in structures, which can help improve design criteria.

The study draws the following conclusions.

- As expected, the R-factor is increased as the height of buildings increases for the reference models with no horizontal eccentricity. A more significant increase is recorded as the height of the building increases. This point concise with previous studies

- The load mechanism failure showed that the increase in horizontal eccentricity causes the column's failure in the direction of eccentricity, while the other columns "in the other direction" are in the elastic state at the same level. This is resulted in non-ductile push-over curves and reduction in R-factor as quantified in the next point
- Having horizontal eccentricity in the building reduced the R-factor as following, given that this reduction is larger for higher structures
  - ✓ For eccentricity indicator ratio < 20-40% of the length, R decreases by negligible percentage "2-5%."
  - ✓ For eccentricity indicator ratio < 50% of the length, R decreases about 10%
  - ✓ For eccentricity indicator ratio < 60% of the length, R decreases about 15%
- The change in R-value may reach 30% when considering the combined effect of flexural, shear-tension, and torsion hinges in series for the extreme torsion irregularity case for the fifteen-story building.
- Structural normalization has an extra reduction of R-value by 3.2% as compared to the non-normalized case for the 15-story building with 0.6L eccentricity

In conclusion, this paper defined the importance of calculating a specific R-factor for RC-IMRF buildings with eccentricity in the design process and offered key insights that can help future seismic design practices and the refinement of building code provisions. As structural engineering evolves all the time, it is necessary to continue studying the effects of torsional irregularity on building behavior to update methods for seismic performance to ensure building safety against earthquakes.

4.3 study limitation

Limitations in the study were present as:

i. High-rise buildings were designed as normal structures, not as special cases.

ii. The building was treated as a Single Degree of Freedom (SDOF) in the pushover analysis, which means only the fundamental mode of vibrational modes was considered. Future research

can analyze more detailed models, like 3D modeling or site-specific seismic considerations, to reach accurate R-factors.

iii. Soil-structure interaction was not considered in the analysis.

iv. Only the effects of horizontal seismic forces were considered in the analysis.

v. effect of shear on the moment-curvature curves, due to the effect of torsion, is ignored

4.4 Future study

The following are some suggestions for future research

- Consider the effect of soil structure interaction on the R-factor.
- Study the impact of eccentricity on the R-factor in a structure with shear walls.
- Determine the R-value of buildings using other non-linear analysis methods, such as time history analysis.
- Evaluate the effect of the eccentricity on the R-factor in the high-rise building.

References

- American Concrete Institute. (2019). The building code requirements for structural concrete are outlined in ACI 318-19, along with commentary provided in ACI 318R-19. ACI Committee 318. Farmington Hills, MI.
- American Society of Civil Engineers. (2016). Minimum design loads and associated criteria for buildings and other structures (ASCE/SEI 7-16). Reston, VA: ASCE.
- ASCE & FEMA. (2000). Prestandard and commentary for the seismic rehabilitation of buildings (FEMA 356). Washington, DC: American Society of Civil Engineers/Federal Emergency Management Agency.
- Applied Technology Council. (1995). Structural response modification factor (ATC-19). Redwood City, CA: ATC.
- Applied Technology Council. (1996). Seismic evaluation and retrofit of concrete buildings (ATC-40). Redwood City, CA: ATC.
- Balaji Rao, A., Srinivas Reddy, P., & Meghana Shaly, C. (2022). Mode shape modification of irregular design of buildings. Materials Today: Proceedings, 62, 1790–1795.
- Cengiz, Ö., & Ünay, A. I. (2005). Residential building architecture in Turkey frequently encounters seismic design flaws. Building and Environment, 42(3), 1406–1416.
- Cheng, X., Chen, Y. Y., & Nethercot, D. A. (2013). Experimental study on H-shaped steel beam-columns with large width–thickness ratios under cyclic bending about the weak axis. Engineering Structures, 49, 264–274.
- Chopra, A. K., & De la Llera, J. C. (2020). Accidental torsion in buildings: Formulation, evaluation, and implications for code provisions. Structures, 28, 2274–2290.
- Computers and Structures, Inc. (2006). SAP2000: Integrated finite element analysis and design of structures. Berkeley, CA: CSI.
- Cuong, N. H., & Kim, S. E. (2009). Practical advanced analysis of space steel frames using fiber hinge method. Thin-Walled Structures, 47(4), 421–430.
- Cuong, N. H., & Kim, S. E. (2012). Practical nonlinear analysis of steel–concrete composite frames using fiber-hinge method. Journal of Constructional Steel Research, 74, 90–97.
- Cuong, N. H., Kim, S. E., & Oh, J. R. (2007). Nonlinear analysis of space steel frames using fiber plastic hinge concept. Engineering Structures, 29(4), 649–657.
- Demir, A. (2010). The torsional irregularity effects of site classes in multiple story structures. International Journal of Research and Reviews in Applied Sciences, 5(1).

- Desmond, T. P., Pekoz, T., & Winter, G. (1981). Edge stiffeners for thin-walled members. Journal of Structural Engineering, 107(2), 173–214.
- Gokdemir, H., Ozbasaran, H., Dogan, M., Unluoglu, E., & Albayrak, U. (2013). Effects of torsional irregularity to structures during earthquakes. Engineering Failure Analysis, 35, 713–725.
- GB. (2002). Technical code of cold-formed thin-wall steel structures. China Planning Press.
- Kim, B. H., & Yun, Y. M. (2010). A second-order inelastic analysis of plane steel frames using a work-increment-control solution technique. Advances in Structural Engineering, 13(6), 1033–1045.
- Kim, S. E., & Lee, J. H. (2001). Improved refined plastic-hinge analysis accounting for local buckling. Engineering Structures, 23(9), 1031–1042.
- Kim, S. E., Park, M. H., & Choi, S. H. (2001). Direct design of three-dimensional frames using practical advanced analysis. Engineering Structures, 23(12), 1491–1502.
- Landge, M. V. (2021). Influence of torsional irregularity on tri-directional floor response spectra used in industrial buildings. Innovative Infrastructure Solutions, 6, 124.
- Maggiano, DiGirolamo, & Lizzi. (2023). Types of structural collapse. Maggiano, DiGirolamo & Lizzi P.S.
- Meenakshi, V. L., Wang, Y., Peng, Y., & Dong, J. (2018). Fiber hinge approach for nonlinear analysis of structural members accounting for local buckling under large deformation. IOP Conference Series: Materials Science and Engineering, 431, 092003.
- National Institute of Standards and Technology. (2017). Guidelines for nonlinear structural analysis for design of buildings. NIST GCR 17-917-46.
- Nurettin, A., Nuray, A., & Fuat, O. (2004). Elastic–plastic stress analysis and expansion of plastic zone in clamped and simply supported thermoplastic-matrix laminated plates with square hole. Composites Science and Technology, 64(8), 1147–1166.
- Omidian, P., & Saffari, H. (2018). Comparative analysis of seismic behavior of RC buildings with shape memory alloy rebar in regular, torsional irregularity and extreme torsional irregularity cases. Journal of Building Engineering, 15, 253–264.
- Ozmen, G. (2004). Excessive torsional irregularity in multi-story structures. Degist, 933–9445.
- Perez, J. C. V., & Montes De Oca, M. M. M. (2017). Assessment of response reduction factors of plan-irregular RC buildings. In Earthquake Resistant Engineering Structures XI (pp. 123–132). WIT Press.

- Rigamonti, D. (2022). Mechanisms of structural failure. Designing Buildings Wiki.
- Shrestha, J. K. (2020). Response reduction factor for masonry buildings. Nepal Journal of Science and Technology, 19(2), 44–50.
- Sun, B., Lu, Y., Wu, S., Li, L., & Huang, X. (2023). Effects of aftershocks on the seismic performances of reinforced concrete eccentric frame structures. Applied Sciences, 13(19), 10767.
- Thai, H. T., Uy, B., & Khan, M. (2015). A modified stress–strain model accounting for the local buckling of thin-walled stub columns under axial compression. Journal of Constructional Steel Research, 111, 57–69.
- Wu, X. X. (2006). Seismic design for multi-story steel frames composed of slender and non-compact sections. Tongji University, 65–80.
- Yacob, A. H. (2022). Determination of the response modification factor (R-factor) of RC moment-resisting frames using nonlinear static pushover analysis considering beam-to-column relative stiffness. An-Najah National University.

Appendices

Appendix A

Thesis figures

Figure A1: Number of natural disaster events according to the International Disaster Database.

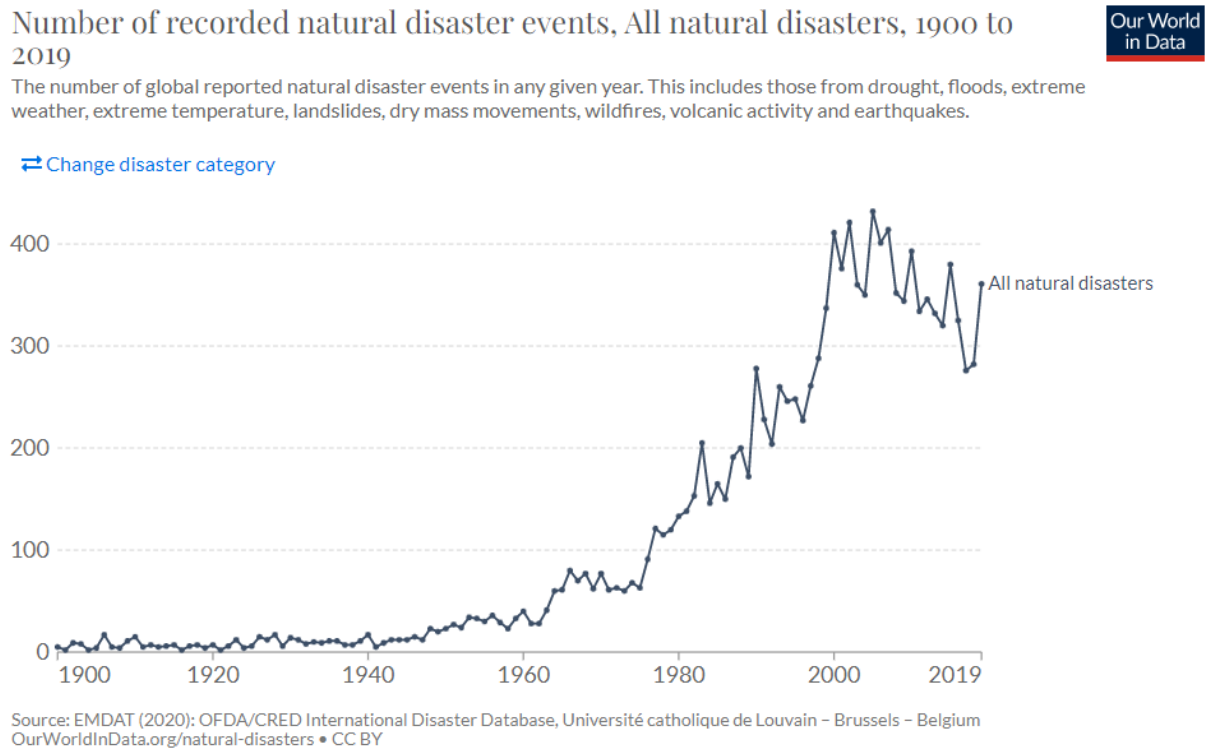

Figure A1: Number of natural disaster events according to the International Disaster Database.

Figure A2: Story drifts simple calculation.

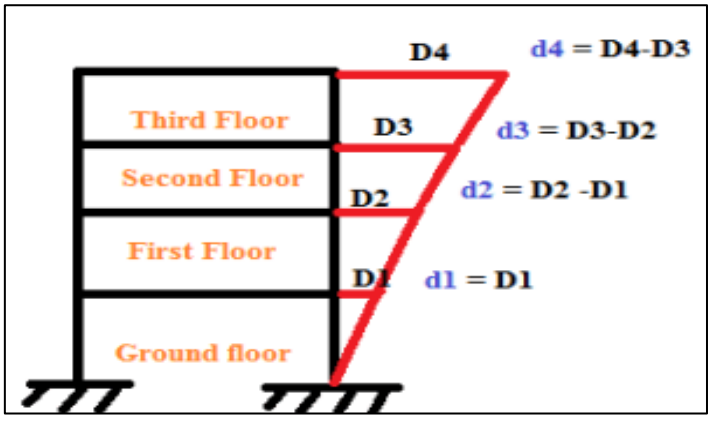

Figure A3: Force displacement response for the structure.

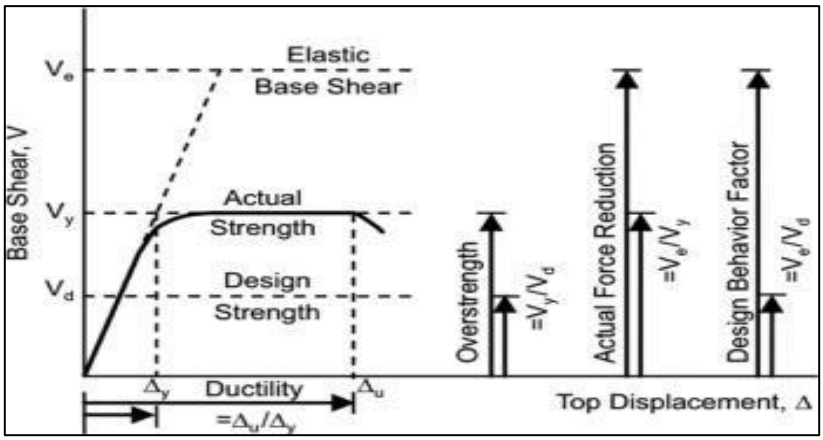

Figure A4: Response reduction factor representation on the force-displacement curve.

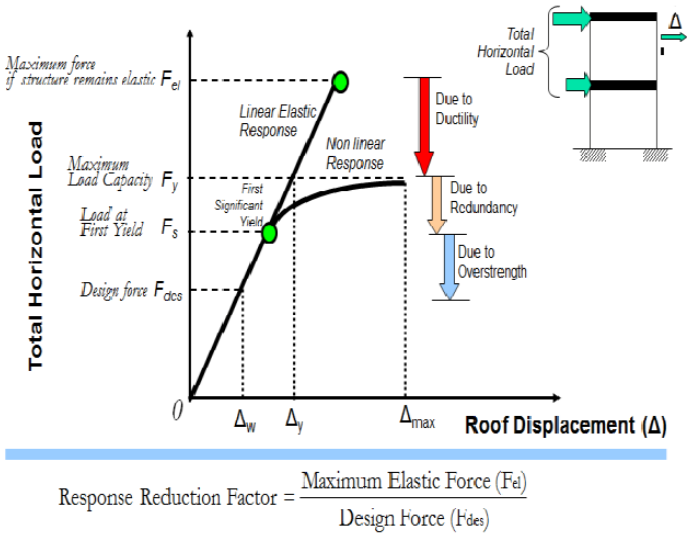

Figure A 5: A beam-column element with a fiber hinge.

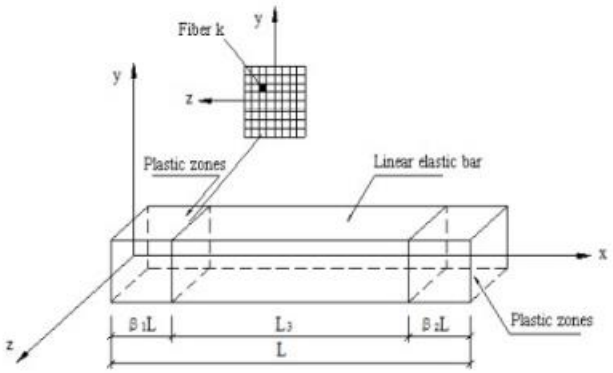

Figure A 6: structure plan view.

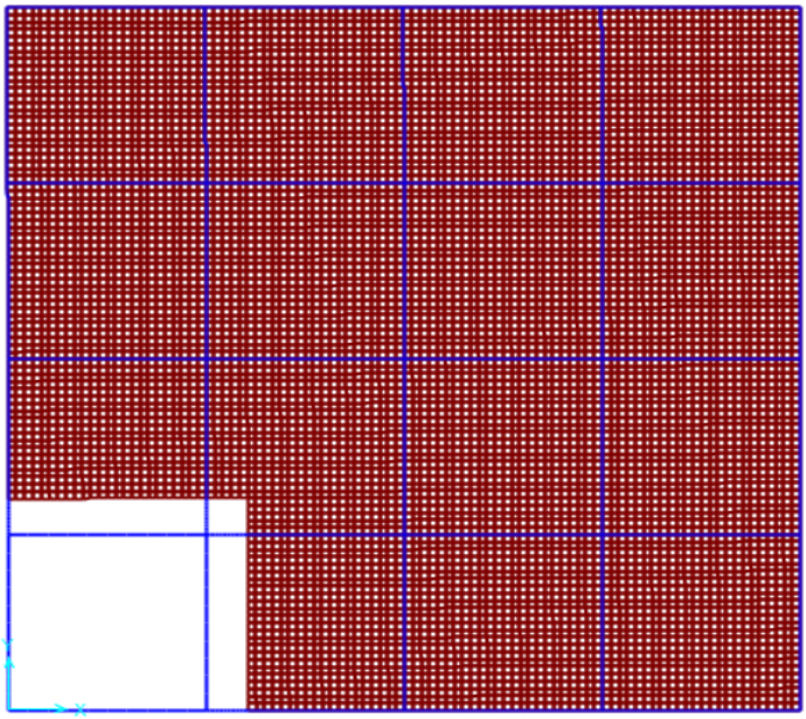

Figure A 7: Structure side view.

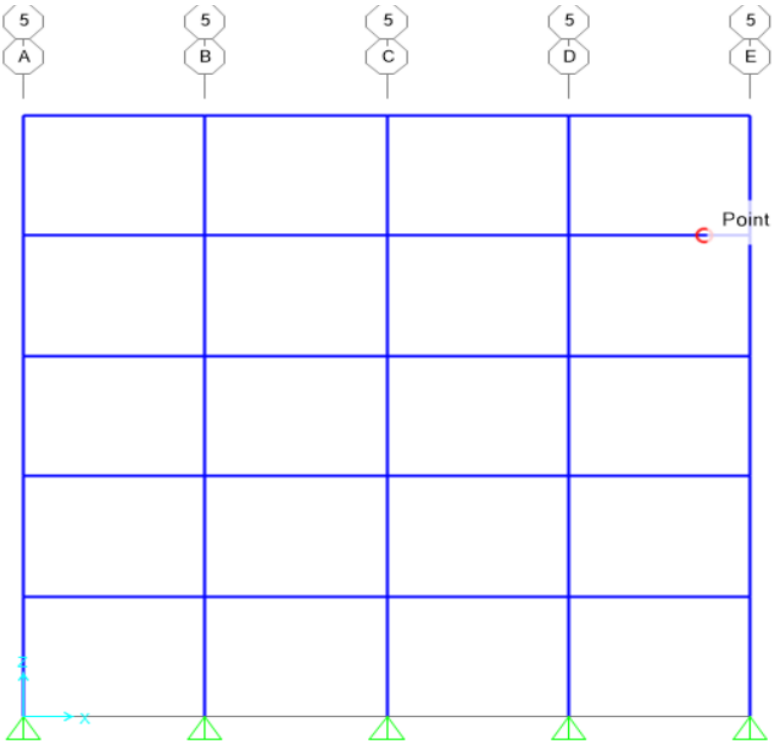

Figure A 8: Case study compatibility check

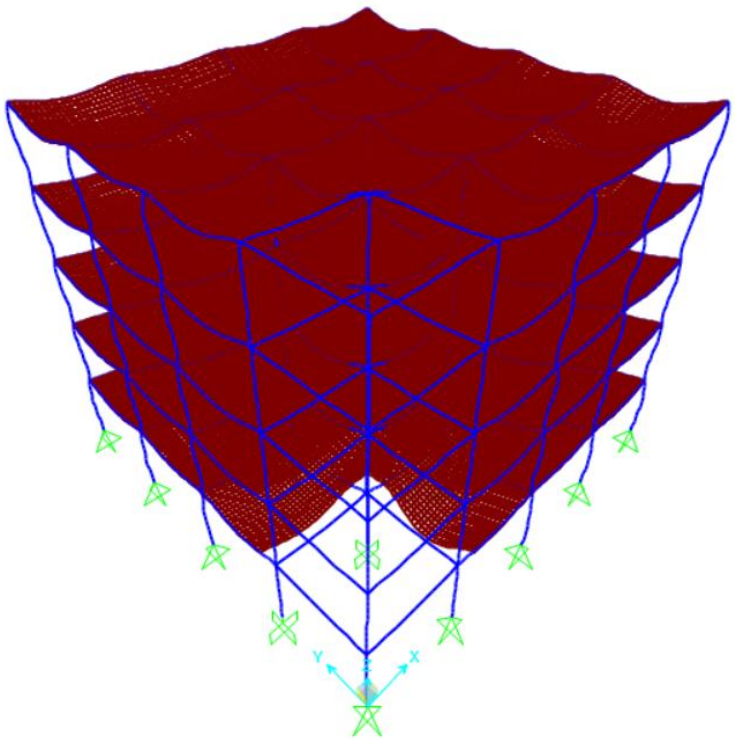

The previous figure demonstrates that the structure's members are well-connected, indicating a successful check.

Figure A 9: Palestinian's seismic hazard map.

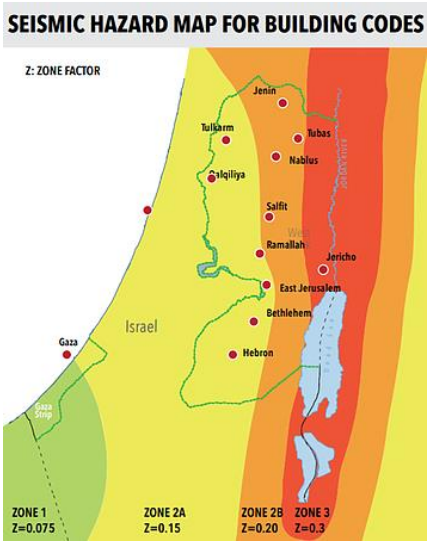

Figure A 10: Redundancy factor in ASCE-07-16 code.

9.5.2.4.1 Seismic Design Categories A, B, and C. For structures in Seismic Design Categories A, B, and C, the value of ρ is 1.0.

Figure A 11: Plastic hinge stages.

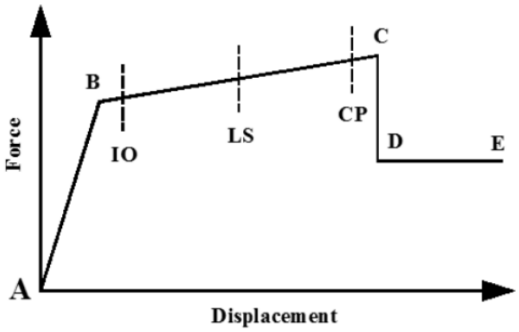

Appendix B
Thesis tables

Table B 1: R-values for moment-resisting frame system in the ASCE code.

Seismic force resisting system	**R**
Steel special moment frames	8
Steel special truss moment frames	7
Steel intermediate moment frames	4.5
Steel ordinary moment frames	3.5
Special reinforced concrete moment frames	8
Intermediate reinforced concrete moment frames	5
Ordinary reinforced concrete moment frames	3
Steel and concrete composite special moment frames	8
Steel and concrete composite intermediate moment frames	5
Steel and concrete composite partially restrained moment frames	6
Steel and concrete composite ordinary moment frames	3
Cold-formed steel —special bolted moment frames	3.5

Table B 2: R-values for moment-resisting system in the UBC-97 code

Basic Structural System	Lateral-Force Resisting system Description	R
Moment-resisting frame System	1. Special moment-resisting frame (SMRF)	
	a. Steel	8.5
	b. Concrete	8.5
	2. Masonry moment-resisting wall frame (MMRWF)	6.5
	3. Concrete intermediate moment-resisting frame (IMRF)	5.5
	4. Ordinary moment-resisting frame (OMRF)	
	a. Steel	4.5
	b. Concrete	3.5
	5. Special truss moment frames of steel (STMF)	6.5

Table B3 shows the R-Factor assigned by the Egyptian seismic code.

Structural System	Ductility	R
RC Moment resisting frame	Sufficient	7
	Not Sufficient	5

Table B 4: Values for modification factor Co.

No. of stories	Co
1	1.0
2	1.2
3	1.3
5	1.4
10	1.5

Table B5: Values for C2.

	T=0.1 sec		T ≥ To	
Structural performance level	Framing type 1	Framing type 2	Framing type 1	Framing type 2
IO	1.0	1.0	1.0	1.0
LS	1.3	1.0	1.1	1.0
CP	1.5	1.0	1.2	1.0

Table B 6: α and β coefficient values as mentioned in Lai and Biggs' study.

Period Range	Coefficient	μ=2	μ=3	μ=4	μ=5
0.1 < T < 0.5	α β	1.6701 0.3291	2.2296 0.7296	2.6587 1.0587	3.1107 1.4307
0.5 < T < 0.7	α β	2.0332 1.5055	2.7722 2.5320	3.3700 3.4217	3.8336 3.8323
0.7 < T < 4.0	α β	1.8409 0.2642	2.4823 0.6605	2.9853 0.9380	3.4180 1.1493

Table B 7: Response factor q_o values according to the Eurocode.

Structural type		q_0
Frame system		5.0
Dual system	Frame equivalent	5.0
	Wall equivalent, with coupled walls	5.0
	Wall equivalent, with uncoupled walls	4.5
Wall system	with coupled walls	5.0
	with uncoupled walls	4.0
Core system		3.5
Inverted pendulum system		2.0

Table B 8 presents the kD value as specified by the Euro-code.

Ductility class	k_D
DC"H"	1.0
DC"M"	0.75
DC"L"	0.5

Table B 9: kR values according to the Euro-code.

Regularity in elevation	k_R
Regular structures	1.0
Non-regular structures	0.8

Table B 10: Table 20.3-1 in ASCE code (Site classification).

Site Class	$\bar{v}_s$	$\bar{N}$ or $\bar{N}_{ch}$	$\bar{s}_u$
A. Hard rock	>5,000 ft/s	NA	NA
B. Rock	2,500 to 5,000 ft/s	NA	NA
C. Very dense soil and soft rock	1,200 to 2,500 ft/s	>50 blows/ft	>2,000 lb/ft^2
D. Stiff soil	600 to 1,200 ft/s	15 to 50 blows/ft	1,000 to 2,000 lb/ft^2
E. Soft clay soil	<600 ft/s	<15 blows/ft	<1,000 lb/ft^2
	Any profile with more than 10 ft of soil that has the following characteristics: — Plasticity index $PI > 20$, — Moisture content $w \geq 40\%$, — Undrained shear strength $\bar{s}_u < 500$ lb/ft^2		
F. Soils requiring site response analysis in accordance with Section 21.1	See Section 20.3.1		

Note: For SI: 1 ft = 0.3048 m; 1 ft/s = 0.3048 m/s; 1 lb/ft^2 = 0.0479 kN/m^2.

Table B 11: VALUES OF Fa AS A FUNCTION OF SITE CLASS AND MAPPED SHORT PERIOD MAXIMUM.

Site Class	Mapped Maximum Considered Earthquake Spectral Response Acceleration at Short Periods				
	$S_S \leq 0.25$	$S_S = 0.5$	$S_S = 0.75$	$S_S = 1.0$	$S_S \geq 1.25$
A	0.8	0.8	0.8	0.8	0.8
B	1.0	1.0	1.0	1.0	1.0
C	1.2	1.2	1.1	1.0	1.0
D	1.6	1.4	1.2	1.1	1.0
E	2.5	1.7	1.2	0.9	0.9
F	*a*	*a*	*a*	*a*	*a*

Table B 12: VALUES OF Fv AS A FUNCTION OF SITE CLASS.

Site Class	Mapped Maximum Considered Earthquake Spectral Response Acceleration at 1-Second Periods				
	$S_1 \leq 0.1$	$S_1 = 0.2$	$S_1 = 0.3$	$S_1 = 0.4$	$S_1 \geq 0.5$
A	0.8	0.8	0.8	0.8	0.8
B	1.0	1.0	1.0	1.0	1.0
C	1.7	1.6	1.5	1.4	1.3
D	2.4	2.0	1.8	1.6	1.5
E	3.5	3.2	2.8	2.4	2.4
F	*a*	*a*	*a*	*a*	*a*

Table B 13: SEISMIC DESIGN CATEGORY BASED ON SHORT.

Value of S_{DS}	Seismic Use Group		
	I	II	III
$S_{DS} < 0.167g$	A	A	A
$0.167g \leq S_{DS} < 0.33g$	B	B	C
$0.33g \leq S_{DS} < 0.50g$	C	C	D
$0.50g \leq S_{DS}$	D[a]	D[a]	D[a]

Table B 14: SEISMIC DESIGN CATEGORY BASED ON 1-SECOND PERIOD RESPONSE ACCELERATIONS

Value of S_{D1}	Seismic Use Group		
	I	II	III
$S_{D1} < 0.067g$	A	A	A
$0.067g \leq S_{D1} < 0.133g$	B	B	C
$0.133g \leq S_{D1} < 0.20g$	C	C	D
$0.20g \leq S_{D1}$	D[a]	D[a]	D[a]

Table B 15: DESIGN COEFFICIENTS AND FACTORS FOR BASIC SEISMIC FORCE-RESISTING SYSTEMS.

Basic Seismic Force-Resisting System	Response Modification Coefficient, R[a]	System Over-strength Factor, W_0[g]	Deflection Amplification Factor, C_d[b]
Ordinary composite reinforced concrete shear walls with steel elements	7	$2\frac{1}{2}$	6
Special reinforced masonry shear walls	7	3	$6\frac{1}{2}$
Intermediate reinforced masonry shear walls	6	$2\frac{1}{2}$	5
Ordinary steel concentrically braced frames	6	$2\frac{1}{2}$	5
Dual Systems with Intermediate Moment Frames Capable of Resisting at Least 25% of Prescribed Seismic Forces			
Special steel concentrically braced frames[f]	$4\frac{1}{2}$	$2\frac{1}{2}$	$4\frac{1}{2}$
Special reinforced concrete shear walls	6	$2\frac{1}{2}$	5
Ordinary reinforced masonry shear walls	3	3	$2\frac{1}{2}$
Intermediate reinforced masonry shear walls	5	3	$4\frac{1}{2}$
Composite concentrically braced frames	5	$2\frac{1}{2}$	$4\frac{1}{2}$
Ordinary composite braced frames	4	$2\frac{1}{2}$	3
Ordinary composite reinforced concrete shear walls with steel elements	5	3	$4\frac{1}{2}$
Ordinary steel concentrically braced frames	5	$2\frac{1}{2}$	$4\frac{1}{2}$
Ordinary reinforced concrete shear walls	$5\frac{1}{2}$	$2\frac{1}{2}$	$4\frac{1}{2}$
Inverted Pendulum Systems and Cantilevered Column Systems			
Special steel moment frames	$2\frac{1}{2}$	2	$2\frac{1}{2}$
Ordinary steel moment frames	$1\frac{1}{4}$	2	$2\frac{1}{2}$
Special reinforced concrete moment frames	$2\frac{1}{2}$	2	$1\frac{1}{4}$
Structural Steel Systems Not Specifically Detailed for Seismic Resistance	3	3	3

Table B 16: COEFFICIENT FOR UPPER LIMIT ON CALCULATED PERIOD

Design Spectral Response Acceleration at 1 Second, S_{D1}	Coefficient C_u
≥ 0.4	1.4
0.3	1.4
0.2	1.5
0.15	1.6
0.1	1.7
≤ 0.05	1.7

Table B 17: VALUES OF APPROXIMATE PERIOD PARAMETERS Ct AND x.

Structure Type	C_t	x
Moment resisting frame systems of steel in which the frames resist 100% of the required seismic force and are not enclosed or adjoined by more rigid components that will prevent the frames from deflecting when subjected to seismic forces	0.028(0.068)[a]	0.8
Moment resisting frame systems of reinforced concrete in which the frames resist 100% of the required seismic force and are not enclosed or adjoined by more rigid components that will prevent the frame from deflecting when subjected to seismic forces	0.016(0.044)[a]	0.9
Eccentrically braced steel frames	0.03(0.07)[a]	0.75
All other structural systems	0.02(0.055)	0.75

Appendix C
Modeling design

- Table C1 displays the densities of typical building materials as per the Jordanian code (JC, 2006) for both forces and loads.

Table C1: Densities of typical materials used in Palestine

Material type	Density (KN/m^3)
Tiles	24
Reinforced concrete	25
Plastering	22
Mortars	22
Fill materials (fine aggregate)	18

The most common thicknesses for materials covered by the slab in Palestine:

- The thickness of tile: 3 cm
- The thickness of mortar: 2 cm
- fills under the tiles: 10 cm
- The thickness of plaster: 1.5 cm

The SID is determined as the following:

$$SID=0.03\times24+0.02\times22+0.1\times18+0.015\times22$$

$$\therefore SID=3.29\ KN/m^2 \rightarrow \text{use } 4\ KN/m^2$$

- The service combinations

- 1.4D×L
- 1.2D + 1.6L.L
- D.L+0.7EQ
- D.L+0.75L.L+0.525EQ
- 0.6D. L+0.7EQ

- Strength combinations

- 1.4D×L
- 1.2D + 1.6L.L
- 1.2D. L+EQ+L.L
- 0.9D. L+EQ
- D.L+0.7EQ
- D.L+0.75L.L+0.525EQ
- 0.6D. L+0.7EQ

- Material properties

The structural frame elements are constructed using reinforced concrete with a unit weight of 25 KN/m3. The strength of the concrete is determined using the code equation for M-24 grade. The elastic modulus of concrete (E_c) is determined as follows:

$$Ec = 4700 \sqrt{f'c} \text{ Mpa} \quad (3.1.1)$$

Where,

f'_c is the concrete compressive strength in Mpa at 28 days, which equals 24 for the M-24 grade.

The steel is ASTM Grade 60. Steel yield strength (f_y) is 420 Mpa, and the modulus of elasticity of steel (E_c) is 2×105 Mpa.

- 3.3.2 Gravity loads

The live loads were taken according to ASCE codes to achieve the minimum requirements. And the superimposed dead load was determined based on typical finishes in Palestine.

Superimposed load = 4 kN/m^2

Live load = 3 kN/m^2. The live load was adopted as 3 kN/m^2 in accordance to ASCE7 for commercial-rental occupancy.

- The hinges between columns and beams were assigned as fiber hinges, and next some important information was added to have correct hinges.

Table C 2: Seven-story column reinforcement.

Story Number	Column Width (cm)	Column Depth (cm)	Reinforcement
1st	40	40	8Ø16
2nd	35	35	8Ø14
3rd & 4th	30	30	8Ø12
5th	25	25	4014

Table C3: Nine-story column reinforcement.

Story Number	Column Width (cm)	Column Depth (cm)	Reinforcement
1st &2nd &3rd	55	55	12Ø20
4th & 5th & 6th	50	50	12Ø18
7th &8th& 9th	40	40	8Ø16

Table C4: Twelve-story column reinforcement.

Story Number	Column Width (cm)	Column Depth (cm)	Reinforcement
1st & 2nd	60	60	16Ø18
3rd to 8th	55	55	12Ø20
9th to 12th	50	50	12Ø18

Table C 5: Fifteen-story column reinforcement.

Story Number	Column Width (cm)	Column Depth (cm)	Reinforcement
1st &2nd &3rd	65	65	12Ø20
4th to 6th	60	60	16Ø18
7th to 11th	55	55	12Ø18
12th to 15th	50	50	12Ø18

Figure C 1: Fiber hinges definition.

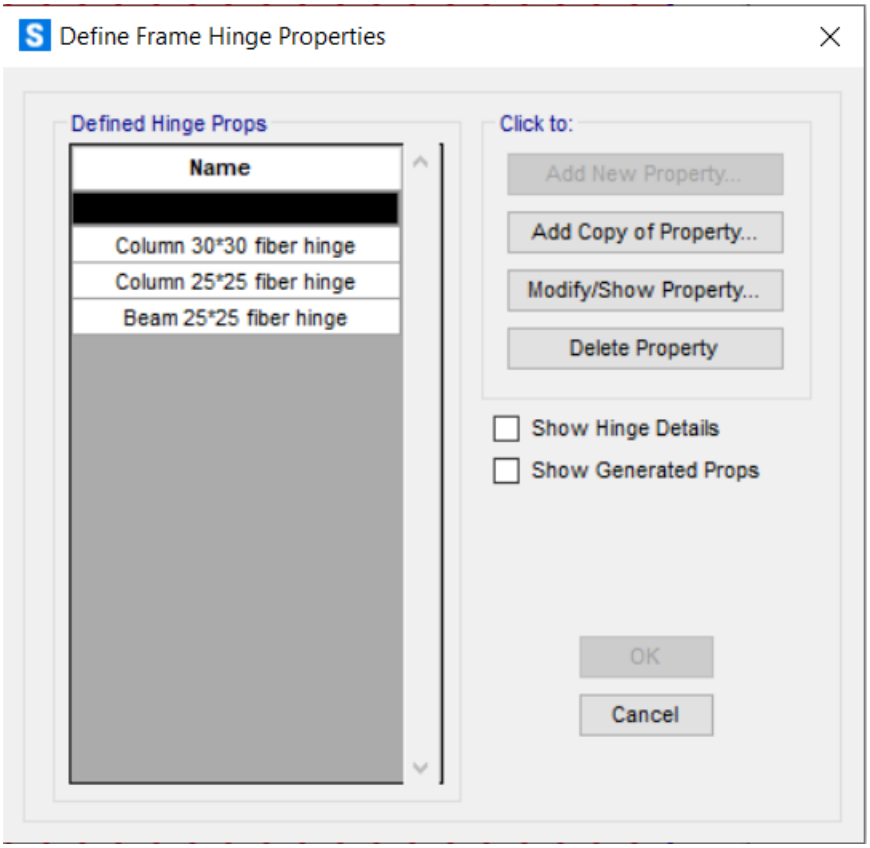

Figure C-2: Fiber hinge property for column 30*30.

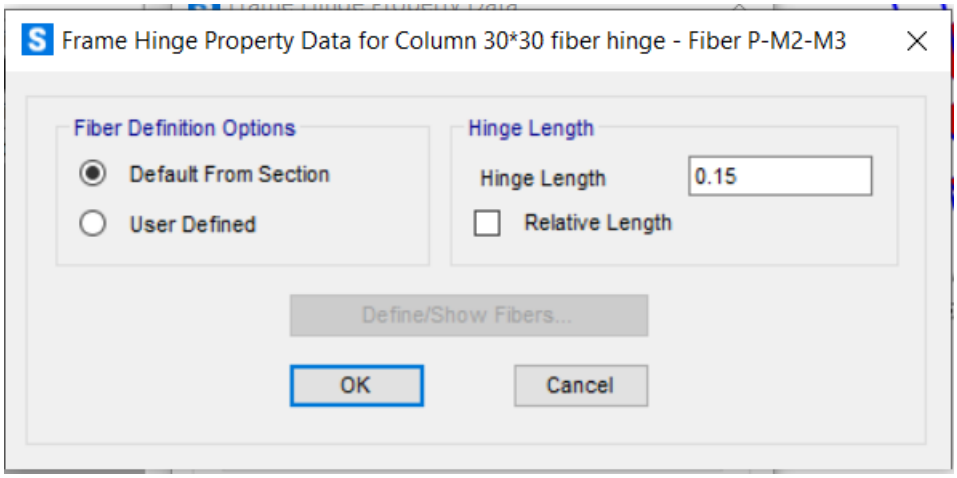

Figure C3: Column section designer.

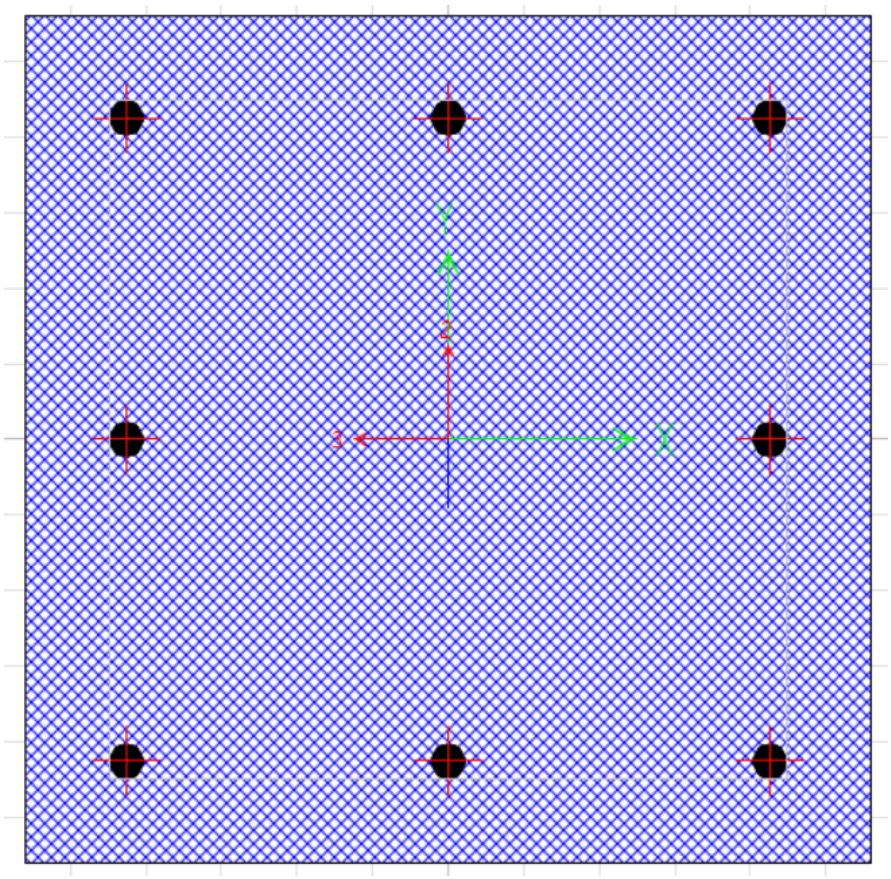

Figure C4: Beam section designer.

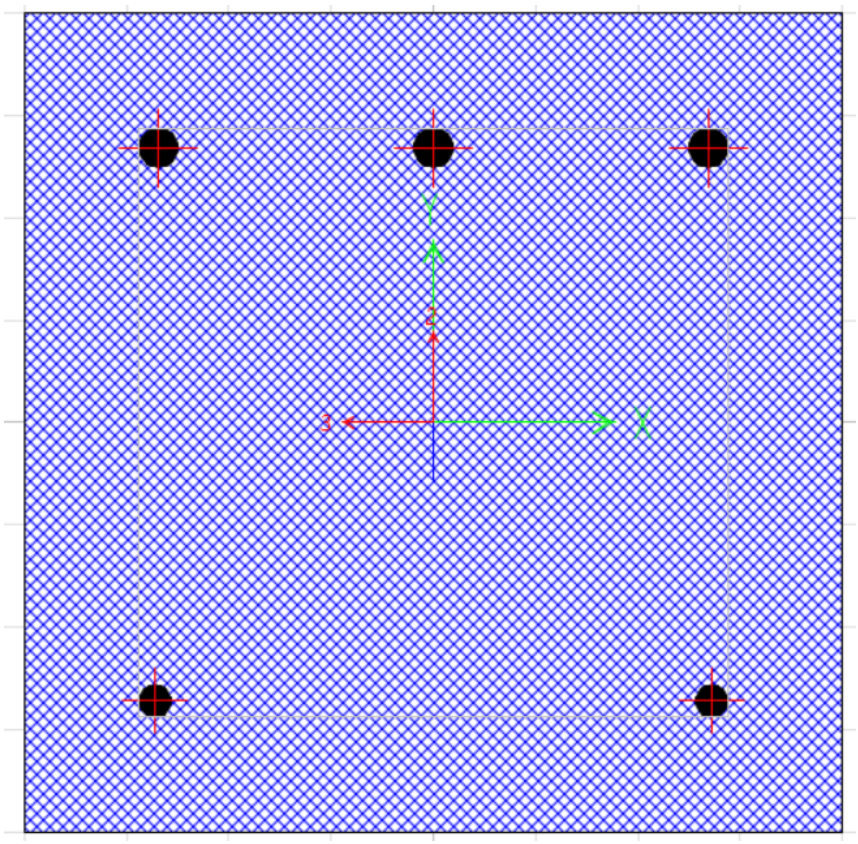

Figure C5: 5: Column's section properties.

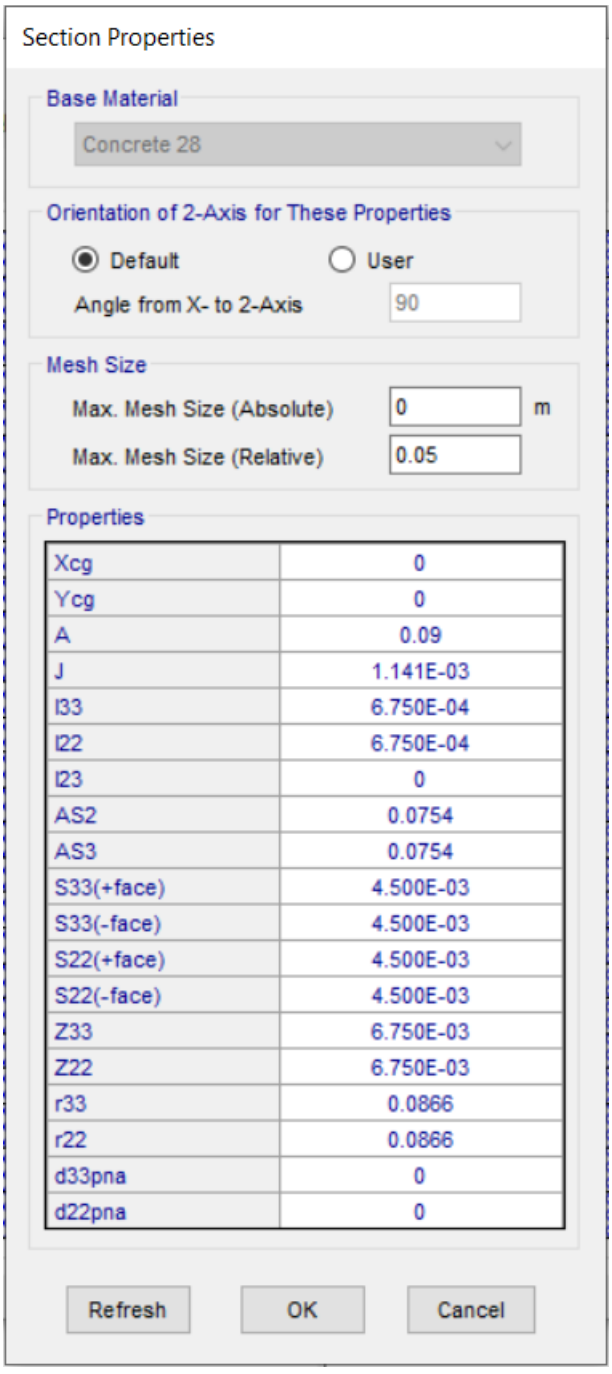

Figure C6: Interaction surface for the column's fiber hinge.

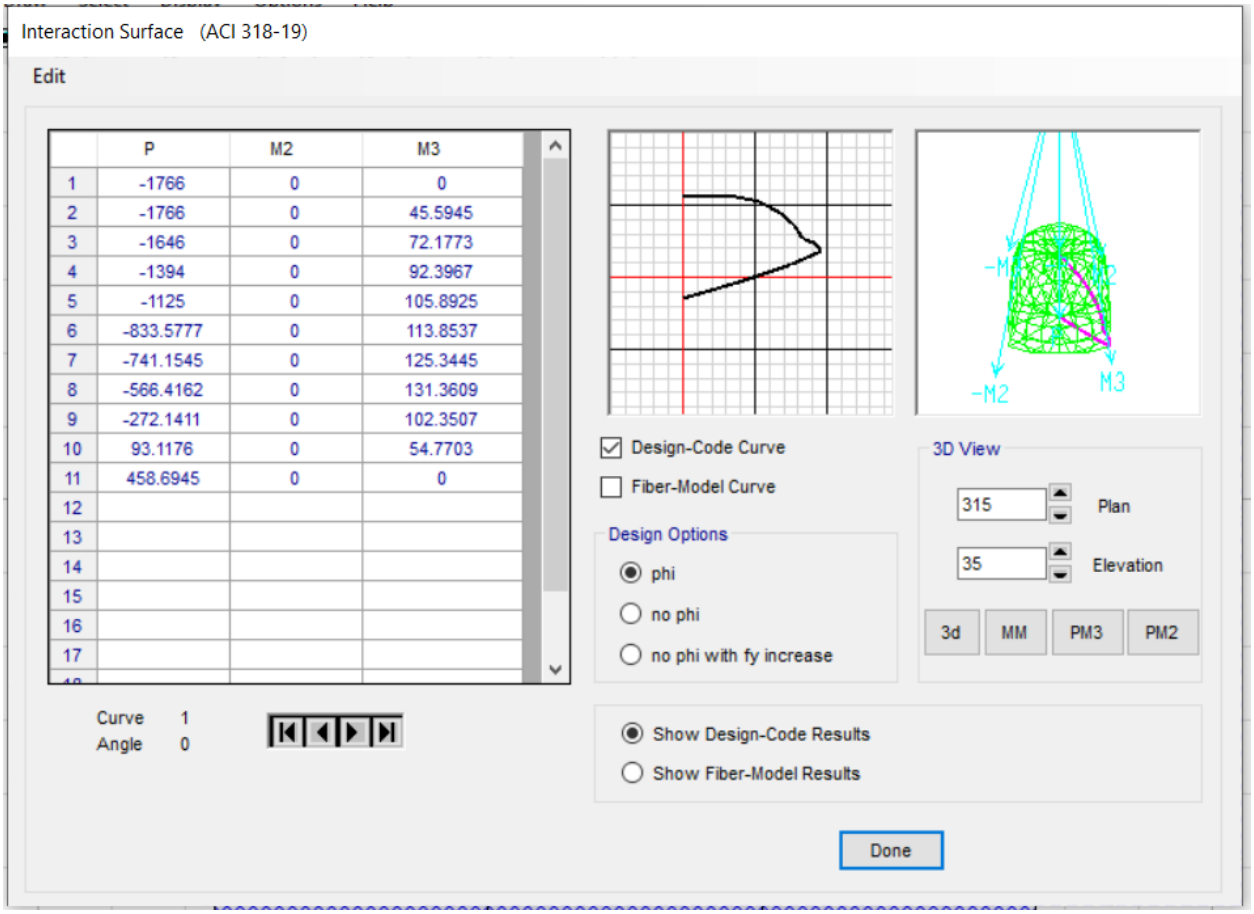

Figure C7: Moment-curvature curve for the column's fiber hinge.

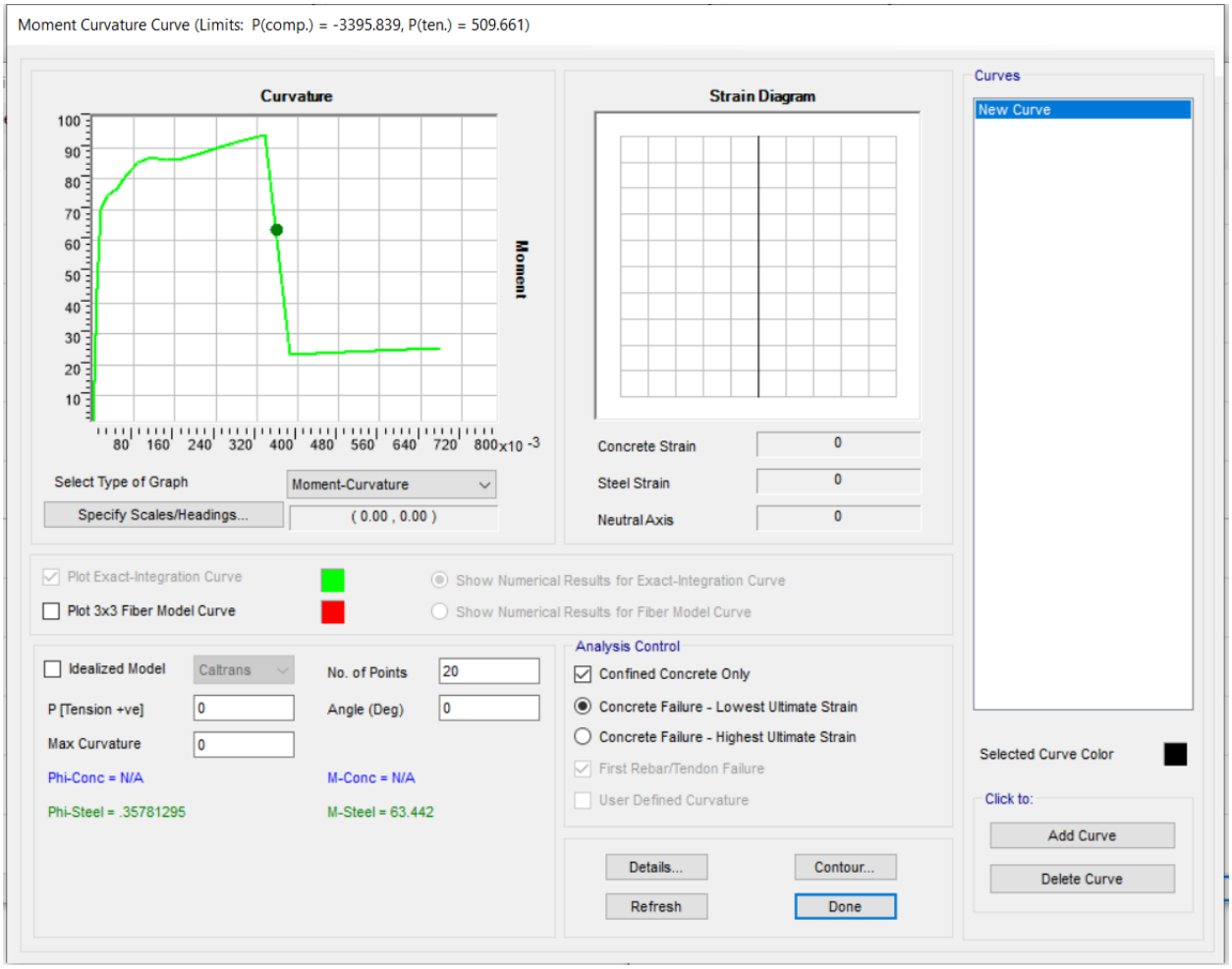

Figure C8: Steel stress-strain curve for the column's fiber hinge.

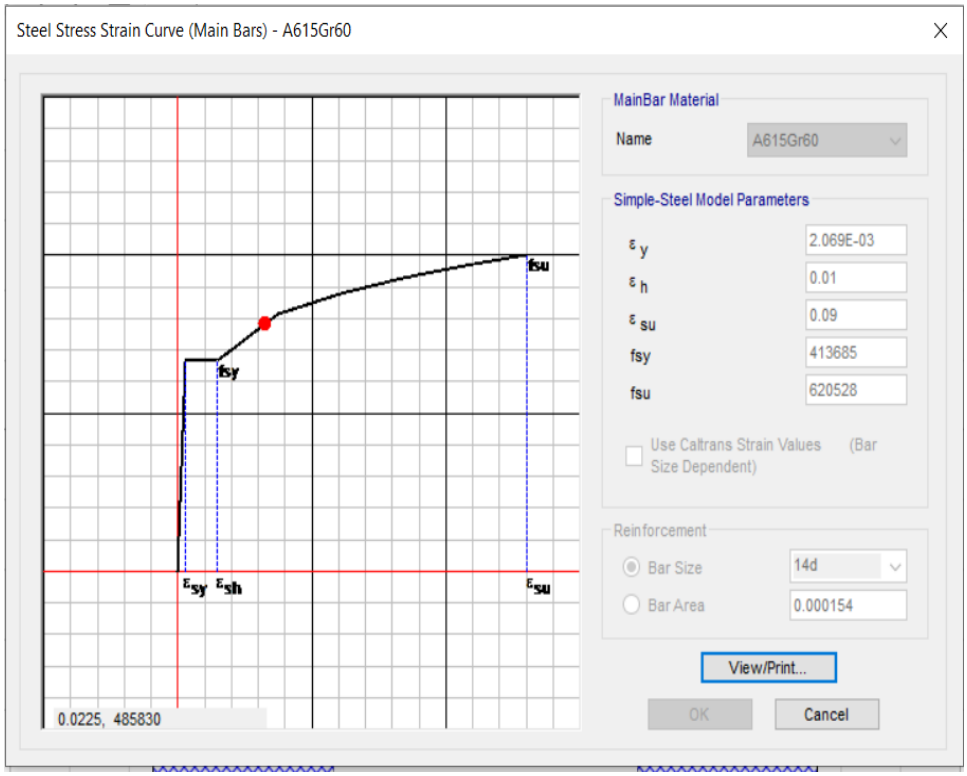

Figure C9: Response spectrum curve definition.

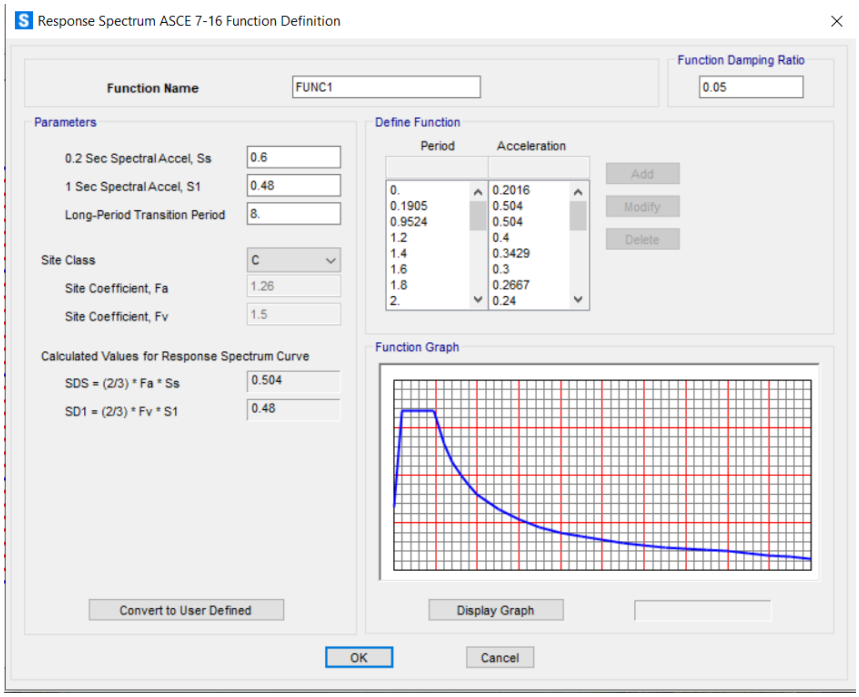

Table C6: Torsional irregularity classification for the structures.

Story	eccentricity indicator ratio	Str. Classification	Story	eccentricity indicator ratio	Str. Classification
5	0	Regular	12	0	Regular
5	0.1	Regular	12	0.1	Regular
5	0.2	Torsional irregularity	12	0.2	Regular
5	0.3	Torsional irregularity	12	0.3	Torsional irregularity
5	0.4	Torsional irregularity	12	0.4	Torsional irregularity
5	0.5	Torsional irregularity	12	0.5	Torsional irregularity
5	0.6	Extreme torsional	12	0.6	Extreme torsional
7	0	Regular	15	0	Regular
7	0.1	Regular	15	0.1	Regular
7	0.2	Regular	15	0.2	Regular
7	0.3	Torsional irregularity	15	0.3	Torsional irregularity
7	0.4	Torsional irregularity	15	0.4	Torsional irregularity
7	0.5	Torsional irregularity	15	0.5	Extreme torsional
7	0.6	Torsional irregularity	15	0.6	Extreme torsional
9	0	Regular			
9	0.1	Regular			
9	0.2	Torsional irregularity			
9	0.3	Torsional irregularity			
9	0.4	Torsional irregularity			
9	0.5	Extreme torsional			
9	0.6	Extreme torsional			

Table C7: 5-stories drift check for 0L and 0.6L eccentricity indicator cases

0L					0.6 L				
Story	δ (cm)	Story drift (cm)	Drift limit	Check	Story	δ (cm)	Story drift (cm)	Drift limit	Check
5	6.98	0.68	6	Ok	5	6.52	0.62	6	Ok
4	6.3	1.2	6	Ok	4	5.9	1.11	6	Ok
3	5.1	1.6	6	Ok	3	4.79	1.46	6	Ok
2	3.5	1.5	6	Ok	2	3.33	1.36	6	Ok
1	2	2	6	Ok	1	1.97	1.97	6	Ok

Table C 8: 7-stories drift check for 0L and 0.6L eccentricity indicator cases

0L					0.6 L				
Story	δ (cm)	Story drift (cm)	Drift limit	Check	Story	δ (cm)	Story drift (cm)	Drift limit	Check
7	7.55	0.59	6	Ok	7	6.88	0.54	6	Ok
6	6.96	1.05	6	Ok	6	6.34	0.85	6	Ok
5	5.91	1.13	6	Ok	5	5.49	1.13	6	Ok
4	4.78	1.34	6	Ok	4	4.36	1.23	6	Ok
3	3.44	1.47	6	Ok	3	3.13	1.34	6	Ok
2	1.97	1.23	6	Ok	2	1.79	1.13	6	Ok
1	0.74	0.74	6	Ok	1	0.66	0.66	6	Ok

Table C9: 9-stories drift check for 0L and 0.6L eccentricity indicator cases

0L					0.6 L				
Story	δ (cm)	Story drift (cm)	Drift limit	Check	Story	δ (cm)	Story drift (cm)	Drift limit	Check
9	7.7	0.4	6	Ok	9	7.4	0.4	6	Ok
8	7.3	0.67	6	Ok	8	7	0.63	6	Ok
7	6.63	0.94	6	Ok	7	6.37	0.91	6	Ok
6	5.69	0.94	6	Ok	6	5.46	0.92	6	Ok
5	4.75	1.06	6	Ok	5	4.54	1.02	6	Ok
4	3.69	1.12	6	Ok	4	3.52	1.09	6	Ok
3	2.57	1.12	6	Ok	3	2.43	1.07	6	Ok
2	1.45	0.97	6	Ok	2	1.36	0.91	6	Ok
1	0.48	0.48	6	Ok	1	0.45	0.45	6	Ok

Table C 10: 12-stories drift check for 0L and 0.6L eccentricity indicator cases

0L					0.6 L				
Story	δ (cm)	Story drift (cm)	Drift limit	Check	Story	δ (cm)	Story drift (cm)	Drift limit	Check
12	13.98	0.36	6	Ok	12	14.06	0.36	6	Ok
11	13.62	0.53	6	Ok	11	13.7	0.54	6	Ok
10	13.09	0.72	6	Ok	10	13.16	0.72	6	Ok
9	12.37	0.9	6	Ok	9	12.44	0.91	6	Ok
8	11.47	1.04	6	Ok	8	11.53	1.04	6	Ok
7	10.43	1.17	6	Ok	7	10.49	1.18	6	Ok
6	9.26	1.27	6	Ok	6	9.31	1.28	6	Ok
5	7.99	1.36	6	Ok	5	8.03	1.37	6	Ok
4	6.63	1.44	6	Ok	4	6.66	1.45	6	Ok
3	5.19	1.55	6	Ok	3	5.21	1.57	6	Ok
2	3.64	1.64	6	Ok	2	3.64	1.65	6	Ok
1	2	2	6	Ok	1	1.99	1.99	6	Ok

Table C 11: 15-stories drift check for 0L and 0.6L eccentricity indicator cases

0L					0.6 L				
Story	δ (cm)	Story drift (cm)	Drift limit	Check	Story	δ (cm)	Story drift (cm)	Drift limit	Check
15	17.77	0.35	6	Ok	15	18.78	0.37	6	Ok
14	17.42	0.52	6	Ok	14	18.41	0.52	6	Ok
13	16.9	0.69	6	Ok	13	17.89	0.69	6	Ok
12	16.21	0.85	6	Ok	12	17.2	0.86	6	Ok
11	15.36	1	6	Ok	11	16.34	1	6	Ok
10	14.36	1.12	6	Ok	10	15.34	1.12	6	Ok
9	13.24	1.23	6	Ok	9	14.22	1.22	6	Ok
8	12.01	1.33	6	Ok	8	13	1.32	6	Ok
7	10.68	1.37	6	Ok	7	11.68	1.38	6	Ok
6	9.31	1.33	6	Ok	6	10.3	1.34	6	Ok
5	7.98	1.38	6	Ok	5	8.96	1.39	6	Ok
4	6.6	1.46	6	Ok	4	7.57	1.46	6	Ok
3	5.14	1.48	6	Ok	3	6.11	1.5	6	Ok
2	3.66	1.64	6	Ok	2	4.61	1.63	6	Ok
1	2.02	2.02	6	Ok	1	2.98	2.98	6	Ok

Table C 12: Torsional irregularity check for 9-story structure.

Story number	Max drift	Average drift	Ratio
Story 9	13.9	11.7	1.188
Story 8	16.3	13.5	1.207
Story 7	18.9	15.8	1.197
Story 6	22.1	18.5	1.195
Story 5	25.6	21.3	1.202
Story 4	30.1	25.0	1.204
Story 3	35.4	29.3	1.208
Story 2	41.2	34.1	1.208
Story 1	76.5	63.3	1.208

Table C 13: Torsional irregularity check for 15-story structure.

Story number	Max drift	Average drift	Ratio
Story 15	9.3	7.8	1.192
Story 14	10.5	8.8	1.193
Story 13	11.7	9.8	1.194
Story 12	13.2	11	1.2
Story 11	15.0	12.5	1.2
Story 10	17.1	14.2	1.204
Story 9	19.6	16.2	1.21
Story 8	22.2	18.3	1.213
Story 7	25.3	20.8	1.216
Story 6	28.7	23.6	1.216
Story 5	32.6	26.8	1.217
Story 4	37.1	30.5	1.216
Story 3	42.3	34.9	1.212
Story 2	48.5	40	1.213
Story 1	88.2	73	1.208

Table C 14: Torsional irregularity check for 15-story structures with 0.6L eccentricity.

Story number	Max drift	Average drift	Ratio
Story 15	10.8	8.4	1.286
Story 14	12.4	9.6	1.292
Story 13	14	11	1.273
Story 12	16.1	12.6	1.278
Story 11	18.6	14.4	1.292
Story 10	21.4	16.6	1.289
Story 9	24.5	19	1.289
Story 8	28	21.7	1.291
Story 7	32	24.8	1.29
Story 6	36.5	28.3	1.291
Story 5	41.6	32.2	1.292
Story 4	47.3	36.7	1.289
Story 3	53.7	41.7	1.287
Story 2	60.8	47.2	1.289
Story 1	110.4	85.5	1.291

Table C 15: The forces on a 5-stories structure column.

Eccentricity indicator ratio	V (kN)	M (kN.m)	V/M
0L	46.0	66.8	0.688
0.2 L	46.4	67.3	0.689
0.4 L	47.4	69.2	0.68
0.6 L	48.9	75.4	0.65

Table C 16: The forces on the 7-story structure column.

Eccentricity indicator ratio	V (kN)	M (kN.m)	V/M
0L	88.1	157.8	0.688
0.2 L	88.3	158	0.56
0.4 L	88.6	159.8	0.55
0.6 L	90.1	160.3	0.56

Table C 17: The forces on a 9-story structure column.

Eccentricity indicator ratio	V (kN)	M (kN.m)	V/M
0L	332.2	703.1	0.47

0.2 L	370.0	736.5	0.5
0.4 L	396.1	805.8	0.49
0.6 L	410.0	810.5	0.5

Table C 18: The forces on a 12-story structure column.

Eccentricity ratio	V (kN)	M (kN.m)	V/M
0L	438.6	1205.2	0.36
0.2 L	440	1209.98	0.37
0.4 L	463.6	1217	0.38
0.6 L	464	1230.5	0.377

Table C 19: The forces on a 15-story structure column.

Eccentricity ratio	V (kN)	M (kN.m)	V/M
0L	610	1463.5	0.42
0.2 L	614	1469.2	0.42
0.4 L	630.3	1475.4	0.43
0.6 L	636.7	1479.8	0.43

Table C 20 : R-values with and without combined flexural/shear/torsion hinges

No stories	Eccentricity indicator ratio	R without additional hinge	R with additional hinge	Change %
5	0.6	4.43	4.19	5.4%
15	0.6	3.73	3.49	6.4%

جامعة النجاح الوطنية

كلية الدراسات العليا

تأثير الانحراف الأفقي في المبنى على معامل الاستجابة الديناميكية المرنة للهياكل الخرسانية المسلحة

إعداد:

هيا عبدالهادي بسطامي

إشراف :

د.محمد سماعنة

د.منذر دويكات

قدمت هذه الرسالة استكمالا لمتطلبات الحصول على درجة الماجستير في هندسة الإنشاءات بكلية الدراسات العليا في جامعة النجاح الوطنية في نابلس ، فلسطين .

2025

تأثير الانحراف الأفقي في المبنى على معامل الاستجابة الديناميكية المرنة للهياكل الخرسانية المسلحة

إعداد

هيا عبدالهادي بسطامي

إشراف :

د.محمد سماعنة

د.منذر دويكات

الملخص

تتناول هذه الدراسة تأثير اللامركزية الأفقية (عدم الانتظام الالتوائي) على عامل تقليل الاستجابة الزلزالية (R–factor)في الأبنية الخرسانية المسلحة ذات الإطارات المتوسطة المقاومة للعزوم (IMRF) تم إجراء النمذجة والتحليل للأبنية باستخدام برنامج SAP2000 وفق متطلبات الكود الأمريكي ASCE 7–16، حيث تم إنشاء نماذج مختلفة بعدد طوابق متفاوت ونسب لا مركزية أفقية متدرجة تصل إلى 60% من عرض المبنى.

أظهرت النتائج أن قيمة عامل التقليل R تتناقص تدريجيا مع ازدياد اللا مركزية الأفقية، وأن هذا الانخفاض يكون أكثر وضوحاً عند زيادة عدد الطوابق. فبالنسبة للنماذج المرجعية المنتظمة، بقيت قيم R متوافقة مع القيم الموصى بها في الكود (5 للمباني المتوسطة المقاومة للعزوم)، بينما انخفضت القيم بمقدار يتراوح بين 2%إلى 5% بوجود لا مركزية الخفيفة، و 10%إلى 15 % في حالة اللا مركزية المتوسطة، وقد يصل الانخفاض إلى 30% في الحالات الشديدة. كما بينت الدراسة أن توزيع الاحمال على شكل قوة لكل طابق بشكل منفصل في النظام الإنشائي يؤدي إلى انخفاض إضافي مقداره 3.2%في قيمة R للمباني ذات الـ15 طابقاً عند لا مركزية مقدارها 0.6 من طول المبنى.

تؤكد هذه النتائج أهمية إعادة تقييم قيمة عامل تقليل الاستجابة في الأبنية غير المنتظمة أفقياً، إذ إن الاعتماد على القيم الثابتة المعتمدة في الكود قد يؤدي إلى تقدير غير دقيق لأداء المبنى الزلزالي في حال وجود عدم

انتظام أفقي في المبنى. وعليه، توصي الدراسة بأخذ تأثير اللامركزية الأفقية بعين الاعتبار في عمليات التصميم الزلزالي وتطوير معايير الكودات المستقبلية لتحقيق أداء أكثر أماناً وواقعية للمباني المعرضة للزلازل.